NeuroImage 77 (2013) 133–147

Contents lists available at SciVerse ScienceDirect

NeuroImage

journal homepage: www.elsevier.com/locate/ynimg

Impact of acoustic coordinated reset neuromodulation on effective connectivity in a neural network of phantom sound

Alexander N. Silchenko [a,*], Ilya Adamchic [a], Christian Hauptmann [a], Peter A. Tass [a,b]

[a] Institute of Neuroscience and Medicine, Neuromodulation, Research Center Juelich, D-52425, Juelich, Germany
[b] Department of Neuromodulation, University of Cologne, 50924 Cologne, Germany

ARTICLE INFO

Article history:
Accepted 6 March 2013
Available online 22 March 2013

Keywords:
Tinnitus
Coordinated reset neuromodulation
Effective connectivity
Dynamic causal modeling

ABSTRACT

Chronic subjective tinnitus is an auditory phantom phenomenon characterized by abnormal neuronal synchrony in the central auditory system. As recently shown in a proof of concept clinical trial, acoustic coordinated reset (CR) neuromodulation causes a significant relief of tinnitus symptoms combined with a significant decrease of pathological oscillatory activity in a network comprising auditory and non-auditory brain areas. The objective of the present study was to analyze whether CR therapy caused an alteration of the effective connectivity in a tinnitus related network of localized EEG brain sources. To determine which connections matter, in a first step, we considered a larger network of brain sources previously associated with tinnitus. To that network we applied a data-driven approach, combining empirical mode decomposition and partial directed coherence analysis, in patients with bilateral tinnitus before and after 12 weeks of CR therapy as well as in healthy controls. To increase the signal-to-noise ratio, we focused on the good responders, classified by a reliable-change-index (RCI). Prior to CR therapy and compared to the healthy controls, the good responders showed a significantly increased connectivity between the left primary cortex auditory cortex and the posterior cingulate cortex in the gamma and delta bands together with a significantly decreased effective connectivity between the right primary auditory cortex and the dorsolateral prefrontal cortex in the alpha band. Intriguingly, after 12 weeks of CR therapy most of the pathological interactions were gone, so that the connectivity patterns of good responders and healthy controls became statistically indistinguishable. In addition, we used dynamic causal modeling (DCM) to examine the types of interactions which were altered by CR therapy. Our DCM results show that CR therapy specifically counteracted the imbalance of excitation and inhibition. CR significantly weakened the excitatory connection between posterior cingulate cortex and primary auditory cortex and significantly strengthened inhibitory connections between auditory cortices and the dorsolateral prefrontal cortex. The overall impact of CR therapy on the entire tinnitus-related network showed up as a qualitative transformation of its spectral response, in terms of a drastic change of the shape of its averaged transfer function. Based on our findings we hypothesize that CR therapy restores a silence based cognitive auditory comparator function of the posterior cingulate cortex.

Introduction

Chronic tinnitus affects about 10–15% of the general population in industrialized countries (Eggermont and Roberts, 2004). In approximately 1–3 of the population chronic subjective tinnitus is so distressing that it causes severe impairments in the quality of life. It has been estimated that 85% of tinnitus cases are accompanied by hearing loss and that occupational and leisure noise are the greatest factors causing cochlear damage (Axelsson and Prasher, 2000; Hall et al., 2012). In addition, the audiometric signs indicating a deafferentation were also detected in tinnitus patients with normal hearing (Schaette and McAlpine, 2011; Weisz et al., 2006). The mechanism of tinnitus generation still remains unclear. It is generally accepted that most forms of subjective tinnitus are attributable to changes in the central nervous system (Eggermont and Roberts, 2004). One characteristic aspect is deafferentation-induced cortical map reorganization (Muhlnickel et al., 1998; Robertson and Irvine, 1989; Weisz et al., 2007a; Yang et al., 2011). However, in accordance with recent findings, cortical map reorganization alone cannot explain the emergence of tinnitus (Schaette and McAlpine, 2011; Langers et al., 2012; Engineer et al., 2011; Weisz et al., 2006).

Another important phenomenon related to the emergence of tinnitus is pathologically enhanced neuronal synchrony, which was observed both in animal studies (Norena and Eggermont, 2003; Ochi and Eggermont, 1997) and in tinnitus patients (De Ridder et al., 2011; Llinas et al., 1999; Weisz et al., 2005, 2007b). In particular, it was shown that in tinnitus patients alpha band power was

* Corresponding author. Fax: +49 2461612820.
E-mail address: a.silchenko@fz-juelich.de (A.N. Silchenko).

1053-8119/$ – see front matter © 2013 Elsevier Inc. All rights reserved.
http://dx.doi.org/10.1016/j.neuroimage.2013.03.013

significantly reduced, whereas delta band power was significantly increased in temporal regions. Furthermore, tinnitus related distress was correlated with this abnormal pattern of spontaneous activity, in particular, in right temporal and left frontal brain areas (Weisz et al., 2005). In further studies, a significant increase of MEG activity in the gamma band was revealed after onset of pronounced activity in delta band (Weisz et al., 2007b). The neural correlate for the tinnitus pitch percept might be provided by the dynamics of the pitch-selective neurons which are located in a spatially restricted low-frequency cortical region near the anterolateral border of the primary auditory cortex (Bendor and Wang, 2005). This might be the reason of enhancement in efficacy of acoustic treatments, which are recently observed in the cases, when a tinnitus pitch was within the stimulated frequency range (Schaette et al., 2010). Several other studies also confirmed that pathological neuronal synchronization is related to the tinnitus percept (De Ridder et al., 2011; Dohrmann et al., 2007; Kahlbrock and Weisz, 2008). Moreover, the functional interaction between non-auditory and auditory areas, displaying abnormal synchrony, appears to be a central feature underlying tinnitus distress (Schlee et al., 2009a,b). In particular, there is growing evidence that non-auditory areas, e.g., amygdala, cingulate cortex and parahippocampus, play a crucial rule in patients with tinnitus distress (Rauschecker et al., 2010, Leaver et al., 2011; Vanneste et al., 2010). Another important issue concerns the possible role of the dorsolateral prefrontal cortex, which is known to exert early inhibitory modulation of input to primary auditory cortex in humans (Knight et al., 1989) and associated with auditory attention (Alain et al., 1998; Lewis et al., 2000; Mitchell et al., 2005; Voisin et al., 2006). For this reason, dorsolateral prefrontal cortex was chosen as a target for transcranical direct current stimulation (tDCS) for the treatment of tinnitus (Vanneste et al., 2011), major depression (Fregni et al., 2006) or to increase the pain threshold (Boggio et al., 2008).

To specifically counteract tinnitus-related neuronal synchrony, a non-invasive desynchronizing stimulation technique, acoustic coordinated reset (CR) neuromodulation, was used in a recent proof of concept study (Tass et al., 2012a). Acoustic CR neuromodulation is based on the use of short pure tones of different pitch to induce shifted soft phase resets of neuronal oscillations in different tonotopically corresponding target areas which are grouped around the dominant tinnitus pitch. CR neuromodulation is essentially based on fundamental principles of self-organization (Tass, 1999, 2003a,b) and exploits the intimate relationship between neuronal dynamics and connectivity (Yuste and Bonhoeffer, 2004). According to computational studies, CR neuromodulation can shift synchronized neural networks with strong synaptic connectivity to a desynchronized state with weak connectivity due to spike-timing-dependent plasticity (Hauptmann and Tass, 2009; Tass and Hauptmann, 2009; Tass and Majtanik, 2006). As a result, a neural network unlearns pathological connectivity and synchrony, i.e. it undergoes an anti-kindling (Tass and Majtanik, 2006). Computationally, it was shown that CR neuromodulation causes an effective desynchronization and an anti-kindling effect no matter whether CR is delivered directly to the neurons' somata or indirectly to synapse (Popovych and Tass, 2012). Hence, from a theoretical standpoint invasive as well as non-invasive, sensory CR neuromodulation should, in principle, be feasible (Popovych and Tass, 2012; Tass and Popovych, 2012). Moreover, both the acute and long-lasting desynchronizing effects of electrical CR neuromodulation have been verified in animal studies (Neiman et al., 2007; Tass et al., 2009). By the same token, sustained long-lasting after-effects of electrical CR neuromodulation were observed in parkinsonian monkeys (Tass et al., 2012b). Later on, we used the concept of CR neuromodulation to develop a non-invasive, acoustic treatment for subjective tonal tinnitus (Tass et al., 2012a).

The acoustic CR neuromodulation aims at desynchronization of a synchronized focus in the tonotopically organized auditory cortex located in area corresponding to the dominant tinnitus frequency and the belonging tinnitus spectrum (Norena et al., 2002). The CR tones are sequentially delivered with the goal for each tone to cause a phase reset of the pathological slow-wave oscillation in the delta frequency band in a neuronal sub-population, which is tonotopically related to the frequency of the particular CR tone (Popovych and Tass, 2012; Tass et al., 2012a). In a prospective, randomized, single blind, placebo-controlled proof of concept trial in 63 patients with chronic subjective tonal tinnitus (RESET study) CR treatment turned out to be safe and well-tolerated and resulted in a highly significant decrease of tinnitus complaints as measured by Visual Analog Scale (VAS) and tinnitus questionnaire (TQ) scores (Adamchic et al., 2012b,c; Tass et al., 2012a). As follows from the analysis of EEG recordings, after 12 weeks of treatment with acoustic CR neuromodulation pathologically elevated delta and gamma activity were both decreased in a network of brain areas comprising primary and secondary auditory cortices as well as non-auditory, e.g., prefrontal areas (Tass et al., 2012a). Apart from that, the tinnitus-related reduction of alpha activity was reversed and alpha activity re-increased in auditory and prefrontal areas (Tass et al., 2012a). In addition, CR neuromodulation induced a tinnitus pitch change, predominantly lowering tinnitus frequencies, and related changes of neuronal synchrony (Adamchic et al., 2012a; Tass et al., 2012a).

We here study the impact of acoustic CR neuromodulation on the effective connectivity in a neural network underlying tinnitus perception. To reveal such a neural network, we applied a data-driven approach, comprising adaptive filtering via empirical mode decomposition (EMD) and subsequent analysis of causal connectivity by partial directed coherence (PDC) (Silchenko et al., 2010), to the sets of the source signals which were extracted from EEG recordings of healthy controls and tinnitus patients before and after CR treatment. Given the sets of connectivity matrices, we compared effective connectivity in controls and in patients before and after CR neuromodulation. The results of this comparison provided us with the information necessary to build a DCM model, predicting the output of the different loop circuits (Moran et al., 2009). For the DCM approach, it is assumed that the observed responses are caused by interactions among neuronal populations or sources in a model with known neurotransmitters and directed connections (Moran et al., 2009). Importantly, the presence of different types of connections in a DCM model enables a theoretical explanation of an observed abnormal activity from the viewpoint of the balance between excitation and inhibition (Moran et al., 2009). According to a recently proposed model framework, the tinnitus percept involves the coordinated abnormal action of both auditory and non-auditory brain areas, leading to a detuning of an excitatory–inhibitory balance that is reflected in a strong decrease of alpha oscillations (Weisz et al., 2011). It is also known that the level of alpha activity may be viewed as an indicator of the state of the cortical tissue: low levels of alpha mean a state of excitation, whereas high levels of alpha reflect a state of strong inhibition or even possibility of the disengagement of one brain area from others (Klimesch et al., 2007; Weisz et al., 2007a, 2011). This idea is in line with recent experimental findings indicating that a decrease of inhibition may lead to a tinnitogenesis in severe intractable central tinnitus (Shulman, 1995; Shulman and Goldstein, 2006).

Our present study consists of four main steps thereby addressing four basic questions: (i) first, we study whether a network of brain sources, related to our previous studies (Tass et al., 2012a), is tinnitus-related in the sense that (a) tinnitus patients display significant EEG power abnormalities as opposed to healthy controls, and (b) these abnormalities are at least partially reversed due to clinically effective CR therapy. (ii) Do tinnitus patients have a significantly different effective connectivity as opposed to healthy controls? and if so, does CR therapy significantly reverse the abnormal pattern of effective connectivity? To reveal the abnormal patterns in effective connectivity, we used the combined data-driven approach, utilizing the consequent application of empirical mode decomposition (EMD) and partial directed coherence (PDC) to the source signals (Silchenko et al., 2010). (iii) Is there a significant imbalance between excitation and inhibition in the

network of brain sources in tinnitus patients compared to healthy controls? In that case, does CR therapy significantly counteract the excitatory–inhibitory imbalance? This investigation is performed by means of DCM (Moran et al., 2009). (iv) From the overall perspective, does the spectral response of the network of brain sources in tinnitus patients differ significantly from that of the healthy controls? and if so, is there any qualitative transformation of the network's spectral response due to CR therapy? To clarify this, we calculate the transfer function which characterizes the spectral response of the tinnitus network as a whole.

Material and methods

Participants

The current work is based on existing data from patients who were treated with acoustic CR Neuromodulation and participated in a prospective, randomized, single blind, placebo-controlled trial (63 patients in total), performed in Germany between 2009 and 2010 (RESET study, Identifier:NCT00927121; (Tass et al., 2012a)). We selected 28 patients for the present study in accordance with the following criteria: (i) all patients suffered from bilateral chronic subjective tonal tinnitus; (ii) EEG data had to be available for both baseline and the 12 weeks visit; (iii) clinical data, i.e., VAS loudness, VAS annoyance, and TQ scores, had to be available for both baseline and the 12 weeks visit. CR treatment was safe and well-tolerated and resulted in a highly significant decrease of tinnitus symptoms as measured by VAS and TQ scores (Adamchic et al., 2012b,c; Tass et al., 2012a). The patients were further classified using a reliable-change-index (RCI) (Jacobson and Truax, 1991) applied to improvements of TQ scores after 12 weeks of CR and assigned to the group of good responders ($\Delta TQ > 12$) or non-responders ($\Delta TQ < 12$), respectively. A $\Delta TQ > 12$ cut off was selected based on the RCI with the assumption that it separates patients with moderate or good relief of their tinnitus symptoms from non-responders having small or no relief in symptoms (Tass et al., 2012a). In addition, we performed the same recordings and analysis of EEG activity for 16 healthy tinnitus-free control subjects.

Treatment

Patients were stimulated for 12 weeks using a portable acoustic device and comfortable earphones (Tass et al., 2012a). In the RESET study patients were randomly allocated to receive acoustic CR neuromodulation (group $G1 - G4$): $G1(n = 22)$, $G2(n = 12)$, $G3(n = 12)$, $G4(n = 12)$. $G1 - G3$ all received stimulation for 4–6 h per day, whereas $G4$ received stimulation for only 1 hour per day. The basic idea of acoustic CR neuromodulation as well as the structures of stimulation protocols are illustrated by the Fig. 1. Stimulation signals were generated based on a specific formula reflecting the logarithmic tonotopic organization of the auditory cortex and on the matched tinnitus frequency (f_t) with an equal number of tones placed below and above the tinnitus frequency. Stimulation tones had to be perceived by patients as equally loud and just super-threshold. Four tones per cycle were played in random order with three stimulation cycles followed by two silent cycles (more details about the so-called ON–OFF pattern of CR neuromodulation can be found in (Lysyansky et al., 2011)). The four tones are based on a patient specific list of frequencies (Tass et al., 2012a): $G1$, $G3$, $G4$ (f_1 to f_4); $G2$ ($G2$, prior to each cycle four frequencies are chosen from f_1 to f_{12}, with the constraint that each cycle has to contain one frequency from each of the four groups f_1 to f_3, f_4 to f_6, f_7 to f_9, and f_{10} to f_{12}). The stimulation tones are equidistantly placed on a logarithmic scale within the interval $[0.5 \cdot f_t, 2 \cdot f_t]$ for $G1 - G4$. Cycle repetition rate was 1.5 Hz for $G1$, $G2$, $G4$, whereas in $G3$ the rate was harmonized to the patients specific EEG data (Tass, 2003b; Tass et al., 2009). A re-adjustment of stimulation parameters was performed at each visit, provided the matched tinnitus frequency had changed. Visits took place after 1, 4, 8, 12, and 16 weeks. Data for this paper come from baseline and the 12 weeks visit, as EEG recordings for all patients were performed at these visits. At each visit, tinnitus loudness and annoyance were assessed off-stimulation (i.e. at least 2.5 hour after cessation of CR neuromodulation) and consecutively on-stimulation (i.e. 15 min after turning on CR neuromodulation) using a VAS scale for loudness (VAS-L) and annoyance (VAS-A) ranging from 0 to 100. In the present study, we only used the off-stimulation VAS scores, because EEG recordings were performed off-stimulation. A pure tone matching procedure was used to determine the best matching tinnitus pitch (from 100 Hz to 10 kHz). Patients were instructed to match the frequency of a pure tone to the perceived pitch of their tinnitus. During this procedure intensity and frequency of the matching tone were controlled by the patient. Tinnitus matching started either well below or well above the patient's tinnitus frequency. The patient had to adjust the matching tone to his/her tinnitus. Patients had to confirm a best matching pitch at least twice. The matching tone was repeatedly interrupted to facilitate the comparison between matching tone and tinnitus. The group of all 28 patients with bilateral tinnitus included patients from all therapy groups $G1$–$G4$: 10 patients from $G1$, 4 patients from $G2$, 6 patients from $G3$ and 8 patients from $G4$. The group of good responders ($n = 12$) consisted of 6 patients from $G1$, 4 patients from $G3$ and 2 patients from $G4$. Accordingly, the group of non-responders ($n = 16$) consisted of 4 patients from $G1$, 4 patients from $G2$, 2 patients from $G3$ and 6 patients from $G4$. We selected the good responders to increase the signal-to-noise ratio. In more details, we selected those patients who responded well, no matter whether they received an optimal treatment (as patients from $G1$ and $G3$) or a treatment with sub-optimal dosage ($G4$). This enabled us to obtain a sufficiently large number of bilateral tinnitus patients necessary for our statistical analysis. In contrast, given the study design mentioned above, we were unable to determine whether these patients did not respond to CR therapy since they received a sub-optimal treatment with respect to dosage ($G4$) or alignment of CR tones ($G2$).

Data acquisition and pre-processing

Each patient underwent two recording sessions: on day 1 before start of treatment and after 12 weeks, minimum 2.5 h after stopping the last stimulation session. Subjects were instructed to retain from caffeinated beverages on the day of the recording to exclude caffeine induced changes of EEG activity. Patients were seated in upright position in a comfortable chair. EEG recordings were obtained in a dimly lit room in a Faraday cage. EEG data were collected from 128 surface electrodes using a HydroCel Geodesic SensorNet. All electrodes were referenced to Cz. The EEG signals were amplified with the NetAmps 200 amplifier (Electrical Geodesics Inc., Eugene, USA), digitized at 1 kHz and analogous band-pass filtered from 0.1 to 400 Hz. Recordings were performed in the awake state during alternating 2 min intervals with eyes closed and eyes open. The perception of tinnitus was the similar in both cases. For all patients we selected the eyes closed data for further analysis, since they were less affected by artifacts. Photogrammetry was performed for all subjects using Geodesic Photogrammetry System, and the individual head shape was modeled for every subject for each EEG session. The scalp EEG was offline re-referenced to an average reference. Signals were additionally digitally filtered with a 0.8–130 Hz digital filter. Each EEG recording was corrected for blink and eye movements in BESA using the surrogate model approach in BESA (Brain Electrical Source Analysis, MEGIS Software, 5.3 version; Scherg et al., 2002). Recordings were further analyzed in MATLAB (The Mathworks, Natick, MA, USA) using EEGLAB2. All EEG segments that contained large muscle or other artifacts were removed. The mean length of the recordings after artifact correction was 3 min 24 s $\pm$ 23 s. The example of EEG signals which were measured from one of the electrodes, located near the right part of the temporal area

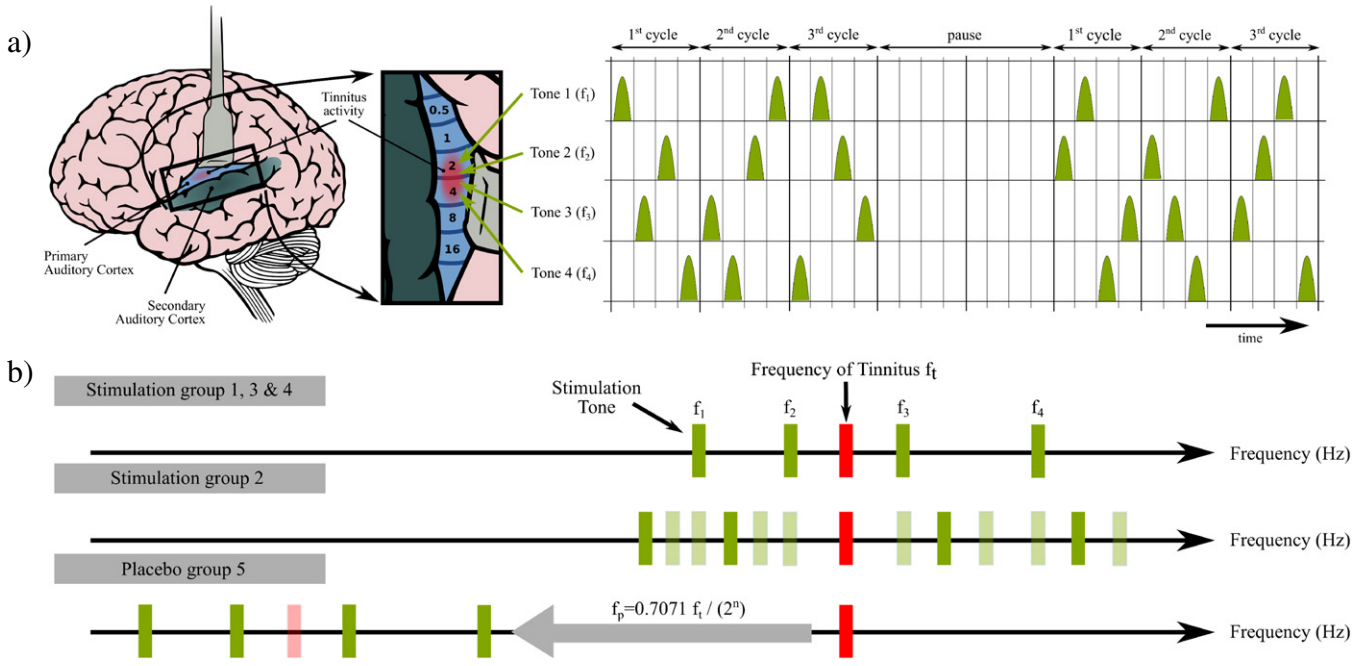

Fig. 1. Acoustic CR neuromodulation: a) The concept of CR neuromodulation comprises a spatial and temporal coordination of the applied stimuli to induce desynchronization (Tass, 2003b): utilizing the tonotopic organization of the primary auditory cortex (left, schematic brain picture adapted from (Chittka and Brockmann, 2005) with kind permission of the authors) short sinusoidal tones of different frequencies (f_1 to f_4) induce a soft reset in different target areas grouped around the dominant tinnitus frequency. Three CR cycles, each comprising a randomized sequence of four tones (right), are followed by two silent cycles. That pattern is repeated periodically. The random variation of the tone sequences (Tass and Majtanik, 2006) and the 3:2 ON–OFF pattern (Lysyansky et al., 2011; Tass, 2003b) optimize the desynchronizing CR effect. b) Four stimulation groups and one placebo group were investigated. For G1, G3 and G4 four tones (top, f_1 to f_4) are grouped around the dominant tinnitus frequency (f_t). G3 differs only in repetition rate F being adapted to the individual EEG δ-band peak. For G2 each CR cycle is formed by a varying composition of four tones (dark green: active) chosen out of twelve tones (middle, f_1 to f_{12}) surrounding f_t. Placebo stimulation (bottom, G5) is formed similar to G1 using a down-shifted stimulation-frequency f_p ($f_p = 0.7071 \cdot f_t/(2^n)$, with n suitably chosen, so that f_p lie within the interval (300 Hz, 600 Hz)) outside the synchronized tinnitus focus. Figure from Tass et al. (2012a) re-printed with permission from the authors, copyright by Forschungscentrum Juelich Gmbh.

A1, before and after CR therapy as well as their power spectra can be found in the Supplementary text.

A source model was generated with regional neural sources placed in the regions of interest (ROI) using BESA. The source montage consisted of temporal (A1, A2, i.e. Brodmann areas BA 41,42), orbito-frontal (OF, BA 11), dorsolateral–prefrontal (DLPFC, BA 9,46) and parietal (PAC, BA 7) sources in both hemispheres, one source was also located within the anterior cingulate cortex (ACC, BA 23) and one in the posterior cingulated cortex (PAC, BA 24). ROIs were defined based on the previous studies (Lanting et al., 2009; Schlee et al., 2009a,b; Vanneste et al., 2011; Weisz et al., 2005). Additional probe-sources were placed in to the occipital lobe and in the area of the central sulcus in both hemispheres. Sources outside the ROIs acted as a spatial filter and reduced the contribution of these regions to the ROI. The strength of the source montages approach is that one can obtain time courses of brain activities from distinct brain regions (Bledowski et al., 2012; Scherg et al., 2002).

To study the effective connectivity in a neural network responsible for the perception of a phantom sound, one, first, has to define the brain areas which are possibly involved. As mentioned in the Introduction Sec.1, the structure of the tinnitus-related network is not yet finally clarified. To get a clue about possible causal connections between different brain areas, we used a model-free data-driven approach to the analysis of EEG source signals. The obtained information was then used to build a "best model" for further DCM analysis. The schematic representation of the whole data analysis procedure is given in Fig. 2.

Data-driven approach to the analysis of effective connectivity

The data-driven approach to the detection of connectivity is based on the combination of EMD and PDC (Silchenko et al., 2010). The main advantage of EMD is that the basis functions are derived directly from the time-series itself, which makes the analysis adaptive, in contrast to the Fourier analysis or wavelet transform, where the basis functions are linear combinations of harmonic functions or wavelets. Indeed, EMD is designed to define a local low frequency component as the local trend, supporting a local high frequency component as a zero-mean oscillation or local detail, so that we can express the signal $s(t)$ as $s(t) = n_1(t) + d_1(t)$. By construction, $d_1(t)$ is an oscillatory signal, and, if it is furthermore required to be locally zero-mean everywhere, it corresponds to an intrinsic mode function (IMF) (Huang et al., 1998). Practically, this primarily implies that all its maxima are positive and all its minima are negative. On the other hand, all we know about $n_1(t)$ is that it locally oscillates more slowly than $d_1(t)$. The recursive decomposition of $n_k(t)$ leads to the following representation of $s(t)$:

$$s(t) = n_K(t) + \sum_{l=1}^{K} d_l(t). \tag{1}$$

The sifting process, providing the separation of fast and slow oscillations, is defined as follows: (i) identify all extrema of $s(t)$; (ii) interpolate two smooth cubic splines between minima and maxima of $s(t)$ to get its upper envelope, $c_{max}(t)$, and its lower envelope, $c_{min}(t)$; (iii) compute the mean $n(t) = (c_{min}(t) + c_{max}(t))/2$; (iv) subtract $n(t)$ from the signal to obtain $r(t) = s(t) - n(t)$. If the stopping criterion is met after l iterations of the sifting process, the local detail and the local trend are defined as $d_1(t) = r^l(t)$ and $n_1 = s(t) - d_1(t)$. The residue n_1 is then treated as a new time-series subject to the sifting process as described above, yielding the second IMF from $n_1(t)$. The procedure continues until either the recovered IMF or the residual time-series are too small (in the sense of the integrals of their absolute values), or the residual time-series has no turning points. Once

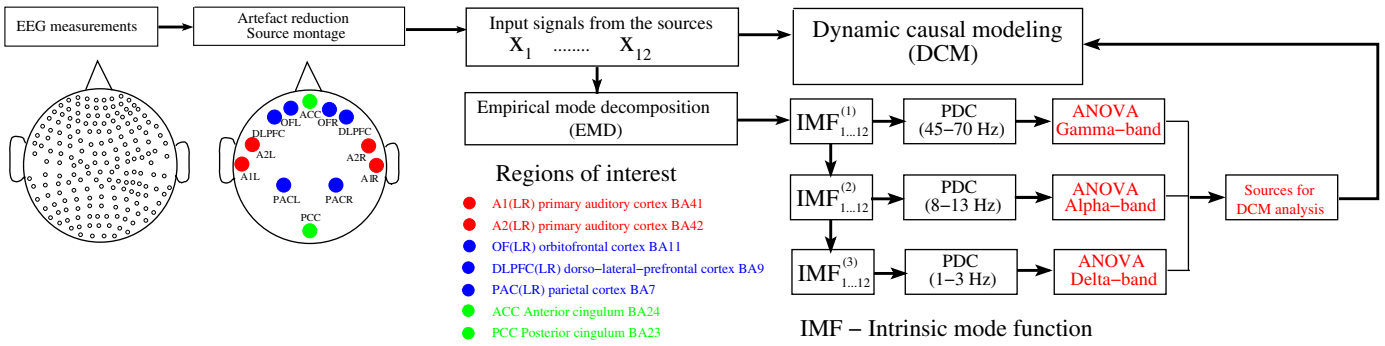

Fig. 2. Schematic diagram illustrating all stages of the acquisition, pre-processing and analysis of EEG data. The sources, comprised in BESA montage, and located in different predefined regions of interest are labeled by the different colors.

all of the wavelike IMFs have been extracted, the final residual component represents the DC component containing the overall trend of the time-series. The details about different algorithms and stopping criteria may be found in (Rilling et al., 2003, 2007). The usage of EMD for each source signals provides a set of IMFs each of which corresponds to one of the co-existing time scales. It allows to avoid drawbacks caused by the prior band pass filtering (Florin et al., 2010) and makes the estimates of directionality of the coupling more accurate (Silchenko et al., 2010).

Given a set of IMFs ($\mathbf{d} = (d_l(t),\ 1 \le l \le K)$) for each of the source signals, one can then use a p-th order autoregressive model (VAR(p)) to estimate effective connectivity in different frequency bands. To attain the effective connectivity in a specific frequency band l, the set of the IMFs $\mathbf{d} = (d_n^l(t),\ 1 \le n \le M)$, calculated for the different source signals, whose power spectra are in the same range may be described as follows

$$\mathbf{d}(t) = \sum_{r=1}^{p} \mathbf{a}(r)\mathbf{d}^l(t-r) + \xi(t), \tag{2}$$

where $\mathbf{a}(r)$ are the matrices whose elements $\mathbf{a}_{ij}$ describe the linear relationship between time series $d_i^l(t)$ and $d_j^l(t)$ at the r-th past lag, M is the total number of sources in a network and $\xi(t)$ is a multivariate Gaussian white noise process with time-invariant positive definite covariance matrix $E(\xi(t),\xi(t)') = \Sigma_\xi$. The dimension of model (2) can be estimated by means of the Akaike criterion, while the values of the coefficients in Eq. (2) can be obtained via the Nuttall–Strand method (Strand, 1977), which is reported to be the best one among multivariate autoregressive estimators (Schlogl, 2006). Then, the spectral domain measure for Granger causality, called partial directed coherence, has been derived from a factorization of the partial spectral coherence and is based on the Fourier transform of the coefficients series (Baccala and Sameshima, 2001; Sameshima and Baccala, 1999):

$$\mathbf{A}(\omega) = I - \sum_{r=1}^{p} \mathbf{a}(r)e^{-i\omega r}. \tag{3}$$

The partial directed coherence from $d_i^l(k)$ to $d_j^l(k)$ in a specified frequency band is defined by:

$$\left|\pi_{i\leftarrow j}(\omega)\right| = |A_{ij}(\omega)| / \sqrt{\sum_k \left|A_{kj}(\omega)\right|^2}, \tag{4}$$

where $0 \le |\pi_{ij}(\omega)|^2 \le 1$ and $\sum_{i=1}^{M} |\pi_{ij}(\omega)|^2 = 1$ for $1 \le j \le M$. Thus, PDC provides a measure for the direct influence of d_j^l to d_i^l via comparison of the linear influence of d_j^l on d_i^l at the frequency ω with the influence of d_j^l on the other variables (Baccala and Sameshima, 2001; Sameshima and Baccala, 1999). After estimation of the PDC, null hypothesis of $\left|\hat{\pi}_{i\leftarrow j}(\omega)\right| = 0$ tests can be performed for each frequency and each IMFs pair at 5%. It can be rejected if the estimated PDC exceeds a threshold value calculated either via an approximation proposed by (Schelter et al., 2005; Schelter et al., 2009) or by the Patnaik approximation of quantile thresholds, utilizing a χ^2_ν distribution with non-integer ν (Silchenko et al., 2010; Takahashi et al., 2007). The maximal values of the partial directed coherence $\pi_{i,j}^{2(max)}$, from which threshold values were subtracted, form a connectivity matrix for a specified set of IMFs.

The above calculations were performed for the good responders and all healthy controls. By using the one-way ANOVA, we compared the elements of connectivity matrices obtained for the controls and tinnitus patients before and after CR stimulation. The results of this comparison for the connectivity matrices in the control group and in the group of good responders before CR treatment allowed us to find the sources, whose interactions were significantly altered by tinnitus. These sources are likely to form a neural network, which is responsible for the perception of a phantom sound. Given the information about the sources forming the tinnitus-related network, one can make the next step by verifying these findings with DCM.

Dynamic causal modeling

DCM is a framework for fitting differential equations to brain imaging data and making inferences about models parameters using Bayesian approach. DCM models predict the output of *in vivo* loop circuits, where observed responses are assumed to be caused by interactions among neuronal populations or sources, with known directed connections and neurotransmitters. Here, we used the Matlab DCM toolbox for steady state responses (SPM8, Wellcome Trust Center for Neuroimaging, London, UK) to fit spectral data features and assess the types of interactions which might be altered by tinnitus (Moran et al., 2007, 2009). The model of each cortical source consists of three (layered) neuronal populations. The differential equations describing neuronal dynamics in brain areas are identical in their form but have different parameters (Moran et al., 2009, 2011). These equations model the postsynaptic convolution of presynaptic inputs by an implicit postsynaptic kernel. The ensemble firing of one population changes the average membrane potential of another, depending on whether it uses glutamate or GABA as a neurotransmitter. Glutamatergic inputs are assumed to produce postsynaptic depolarization, while GABAergic inputs are assumed to produce hyperpolarizing. These effects are mediated by a postsynaptic (alpha) kernel that is either positive or negative, respectively. This (excitatory or inhibitory) influence of one population on another is parameterised by extrinsic connectivity between distinct sources. Thus, effective connectivity is modeled as a gain factor that couples discharge rates in one population to membrane potentials in another (Moran et al., 2009, 2011).

DCM was designed to test hypotheses about the neuronal mechanisms that underlie experimental measurements of brain responses. It allows one to specify a generative model of measured brain data, which is a specific probabilistic mapping from experimentally controlled manipulations via neuronal dynamics to observed data (Stephan et al., 2010). For this reason, Bayesian model selection (BMS) is, usually, the first step in DCM. The models which are compared have to be designed empirically or obtained via model-free testing of Granger causality, as in our case. In BMS, models are usually compared via their Bayes factor, i.e., the ratio of their respective evidences or their difference in log-evidence (relative log-evidence). The chosen model has to explain the data as accurately as possible and, at the same time, has minimal complexity (Stephan et al., 2010). We used BMS for fixed effects to select the best model of interaction for the chosen sources (Stephan et al., 2009). The model with the highest relative probability compared to the other considered models was used to fit the cross-spectral densities for the frequency range 1–90 Hz and to make inference on extrinsic coupling parameters. Then, the significance of effective coupling within the best model was tested via a one-way ANOVA corrected for multiple comparisons to find statistically significant values of coupling exceeding a threshold ($p \leq 0.05$).

Results

Changes in oscillatory activity induced by CR neuromodulation

As a first step in our present study, we compared the levels of oscillatory activity in EEG recordings of the tinnitus patients and healthy controls. To estimate the power of oscillations in gamma, beta, alpha, and delta bands, the short-time Fourier transform was performed for every source signal extracted from EEG recordings of the control subjects and patients before and after CR treatment. The total power of oscillations was calculated over the obtained spectrograms for each of the source signals. Then, all source signals were divided via EMD into the corresponding sets of the IMFs. The energy of each IMF, being calculated via the short-time Fourier transform, gave us a power estimate for a specified frequency band related to that IMF. The normalized power of oscillations in a specified frequency band was estimated as a ratio of the IMF's power and total power of the source signal from which the IMF was extracted. In accordance with the above procedure, the normalized oscillation power was calculated in all frequency bands for all source signals obtained for the patients and for the healthy controls. Then, we compared the values of the normalized power in specified frequency bands obtained for the patients and healthy controls via one-way ANOVA.

The results of this statistical analysis are presented in Fig. 3. As clearly seen, the power spectra of the good responders before CR treatment indicate a significantly enhanced activity in gamma and delta frequency bands together with a strong reduction of power in the alpha band for the sources located in the auditory cortex, cingulate cortex as well as in the frontal area. The oscillatory power in the beta band was also significantly larger than the control values in the areas A1, OFL and PCC before CR treatment. The oscillatory beta activity in the orbitofrontal cortex and posterior cingulate cortex is important for the emotional processing of sounds (Vanneste et al., 2012). As seen from Fig. 3, it was not significantly changed by CR neuromodulation and remained at approximately the same level as compared to the control values.

In the group of good responders, the normalized power of oscillations in A1L, A1R, DLPFCL, DLPFCR and PCC was significantly altered by CR neuromodulation. In more detail, the amplitude of gamma oscillations was significantly altered in the A1L, DLPFCL, and PCC. Alpha power was altered by CR therapy in the A1L, A1R, DLPFCL, DLPFCR and PCC. Remarkably, the levels of gamma and alpha oscillatory activity in these areas after CR therapy were not significantly different from the control values. As further seen from Fig. 3, the amplitude of the synchronized delta oscillations in A1L, DLPFCL and PCC was significantly altered by CR neuromodulation but remained significantly higher as compared to the healthy controls. The latter observations can be explained by the fact that the levels of delta power are negligibly small for healthy controls.

In the case of non-responders, we observed the qualitatively different situation which is characterized by the absence of significant changes in oscillatory power in the gamma and alpha frequency bands after the CR therapy. The changes of the power of low-frequency delta oscillations were observed in areas which are differ from those the above reported for the group of good responders. More details about the changes in power for the group of non-responders can be found in the Supplementary text.

A model-free approach to the detection of a tinnitus network structure

Given the preliminary results about alterations of oscillatory brain activity caused by CR neuromodulation, one may conclude that CR therapy is able to modulate activity in different parts of the brain. Unfortunately, a generic mechanism of tinnitus generation is still unclear. The information about the structure of the tinnitus network, underlying the perception of phantom sound, is not complete and depends on specific method allowing to study different target areas in the brain. In most of the recent studies, utilizing different complementary techniques, the primary auditory cortex, dorsolateral prefrontal cortex, cingulate cortex, amygdala and parahippocampal area were identified as the main elements of the tinnitus network (De Ridder et al., 2011; Rauschecker et al., 2010, Leaver et al., 2011; Schlee et al., 2009a,b; Vanneste et al., 2010). Our above results confirmed a possible involvement of auditory and non-auditory brain areas in tinnitus perception. It is likely that an interaction of auditory and non-auditory brain areas is a key element responsible for the tuning of a balance between excitation and inhibition in the auditory system, whose disruption may lead to the appearance of the coherent low-frequency activity in auditory system and underlay tinnitus perception.

To reveal a causality of interactions between brain areas in which oscillatory activity was altered by CR neuromodulation, we used the above data-driven approach. In accordance with the procedure described in Data-driven approach to the analysis of effective connectivity Sec. 2.4, we calculated the IMFs, corresponding to the different frequency bands, for each of the source signals obtained for all patients and control subjects. As follows from the above analysis, the statistically significant alterations in oscillatory activity induced by CR neuromodulation were found in gamma, alpha and delta frequency bands. The oscillations in these frequency bands are approximated by the IMF2, IMF5 and IMF9, respectively. These modes were further used in the present study to reveal the causality in interaction between sources. As for instance, the second modes (IMF2), calculated for each of the twelve sources, constitute a set of twelve signals describing oscillatory activity in the gamma frequency band. Then, this set of IMF2 was used to detect significant causal connections among sources in the gamma frequency band via the partial directed coherence, as described in Data-driven approach to the analysis of effective connectivity Sec. 2.4. The same calculations were performed for the sets of IMF5, corresponding to the alpha band, and sets of IMF9, describing low-frequency oscillations in delta band. These calculations were performed for all healthy controls and all tinnitus patients. As a result, we got three connectivity matrices, characterizing effective connectivity in the gamma, alpha and delta frequency bands, for each of the control subjects and every patient before and after CR treatment. Thus, each element of the obtained connectivity matrices characterizes the interaction within a pair of sources in one of the three frequency bands specified above. Then, a one-way ANOVA was used to compare the corresponding element $|\pi_{ij}|^2$ of the connectivity matrices calculated for the healthy

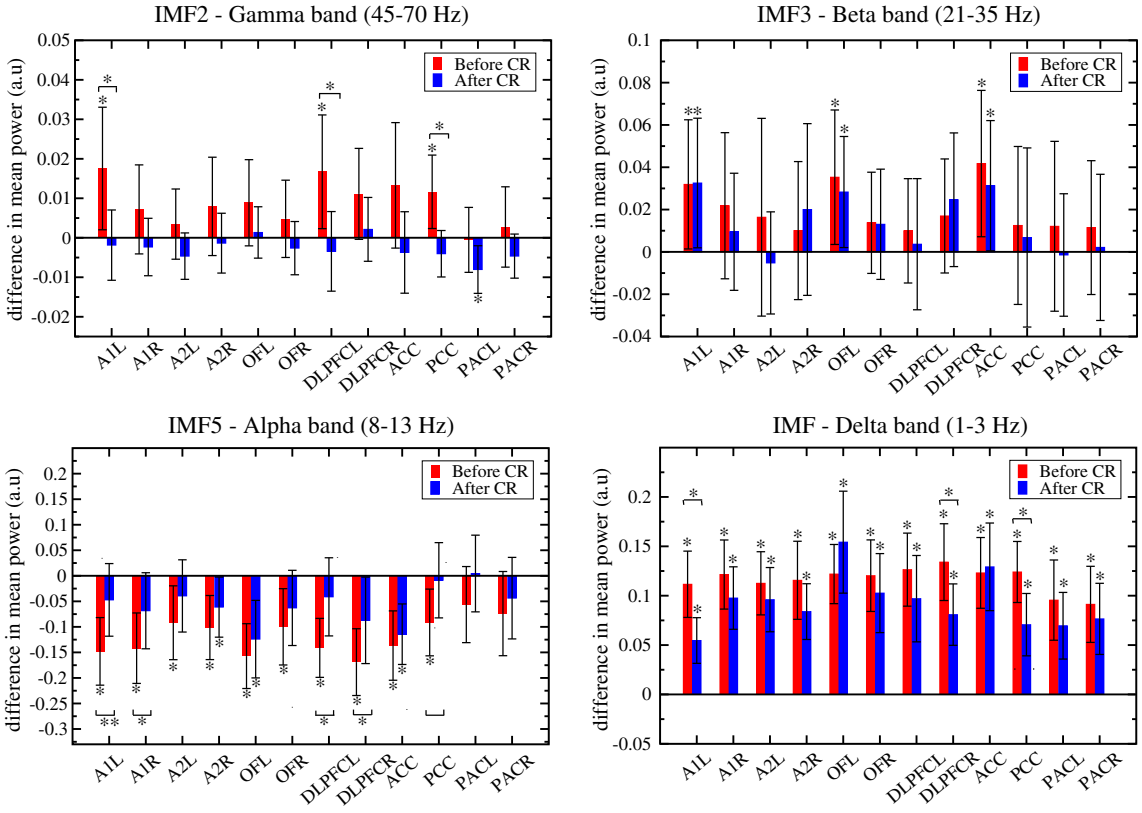

Fig. 3. Deviations of the mean oscillatory power in predefined ROIs from the control values calculated for the good responders before and after CR therapy. The normalized mean oscillatory power in predefined ROIs was calculated via group averaging for the tinnitus patients and for the healthy controls. The values of the mean power obtained for the healthy controls were then subtracted from the values of the mean oscillatory power obtained for the tinnitus patients. The ROIs in which differences were found to be statistically significant (with $p < 0.05$) are labeled by asterisks. The 95% confidence intervals are shown by error bars for each region. The ROIs, where differences of the mean power for the tinnitus patients before and after CR therapy demonstrated statistically significant changes (with $p < 0.05$) are also labeled by asterisks.

controls $|\pi_{ij}^{h}|^2$ and for the tinnitus patients before $|\pi_{ij}^{pb}|^2$ and after $|\pi_{ij}^{pa}|^2$ CR treatment. The further correction for multiple comparisons allowed us to reveal the elements of connectivities matrices, which significantly differ from each other and define measures of changes in effective connectivity as follows:

$$\Delta\varepsilon_{hpb} = \frac{1}{N}\sum_{k=1}^{N}\left(\left|\pi_{ij}^{h}\right|_k^2 - \left|\pi_{ij}^{pb}\right|_k^2\right), \Delta\varepsilon_{pba} = \frac{1}{N}\sum_{k=1}^{N}\left(\left|\pi_{ij}^{pb}\right|^2 k - \left|\pi_{ij}^{pa}\right|_k^2\right), \Delta\varepsilon_{hpa} = \frac{1}{N}\sum_{k=1}^{N}\left(\left|\pi_{ij}^{h}\right|^2 k - \left|\pi_{ij}^{pa}\right|_k^2\right), \tag{5}$$

where $1 \le k \le N$ and N is the number of tinnitus patients in the group of good responders.

The connections whose strengths were significantly different from the control values are schematically drawn in Fig. 4. The sources, whose incoming or outcoming effective connections have strengths significantly different from the control values, were considered as elements of a neural network of phantom sound. For the good responders before CR treatment, the revealed structure of the tinnitus network includes the following areas: A1L, A1R, A2L, A2R, DLPFCL, DLPFCR and PCC. For good responders before CR treatment, we observed a statistically significantly increased strength of interaction between primary auditory cortex and posterior cingulate cortex in gamma and delta frequency bands, while the effective connectivity between dorsolateral prefrontal cortex and temporal areas was altered in the alpha band. As illustrated in Fig. 4, CR stimulation significantly normalizes nearly all initially abnormal connections, which were classified above as "pathologically" altered by tinnitus. This transformation may be considered as a restoration of effective connectivity to its normal "healthy" state. It is necessary to note here that, in the case of non-responders, we had not observed such a restoration of effective connectivity what might be explained either by the sub-optimal dosage of CR neuromodulation or by the large intrinsic differences of the pattern of the functional connectivity prior to therapy. More details about the changes of effective connectivity in the case non-responders can be found in the Supplementary text.

Given the above results indicating the alteration of effective connectivity in the group of good responders after CR therapy we also tested the presence of correlation between changes in effective connectivity and changes in TQ scores. In particular, for those connections, whose coupling strengths were significantly altered after CR therapy we performed regressive analysis to reveal the possible correlations between the observed changes in effective connectivity and changes in TQ scores, whose significant improvements allowed us to classify some patients as good responders (Tass et al., 2012a). The changes in the coupling strength for each of the specified connections $\Delta\varepsilon_{pba}^{k}$ are defined as the difference between the estimates of the coupling strength before and after CR therapy

$$\Delta\varepsilon_{pba}^{k} = \Delta\varepsilon_{pb}^{k} - \Delta\varepsilon_{pa}^{k}, \tag{6}$$

where k is a number of the patient, belonging to the group of good responders. As mentioned above in Sec. 2.1 Participants, the changes in TQ scores are limited from below for the good responders as $\Delta TQ \ge 12$ points. The results of regression analysis, which are presented in Fig. 5, clearly demonstrate the presence of significant correlations for nearly all considered connections, except for the A2R to A2L connection. This fact may be considered as evidence of the influence of acoustic CR neuromodulation on effective connectivity.

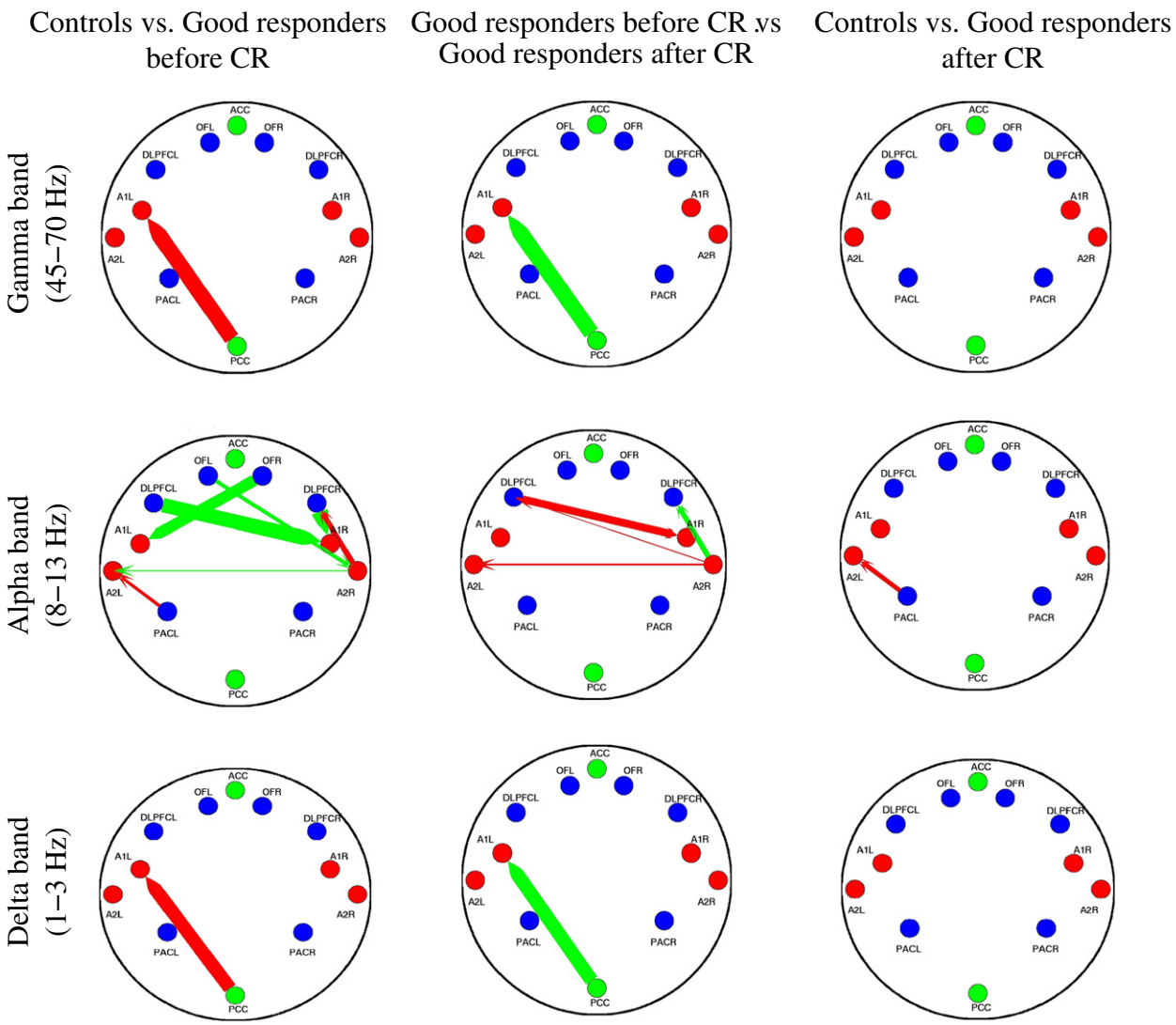

Fig. 4. Schematic representation of the one-way ANOVA results for the differences in effective connectivity calculated for the group of healthy controls and groups of good responders before and after CR neuromodulation. The color of the arrows is defined by the sign of the corresponding measure $\Delta\varepsilon_{hpb}$, $\Delta\varepsilon_{pba}$ or $\Delta\varepsilon_{hpa}$, which are defined in Eq. (5). Red color corresponds to a negative sign of the corresponding measure and means strengthening of interaction between sources, whereas green color corresponds to a positive sign and means weakening of interaction. The width of every arrow is linearly proportional to the corresponding measure defined in Eq. (5). The directionality of interaction is directly defined by the coordinates (i,j) of the element in the connectivity matrices.

The above results, obtained for the group of good responders, gave us preliminary information about the possible structure and causal interactions among brain areas comprised in the tinnitus network. To further hypothesize about the types of the observed interactions, we made a next step and verified our findings by means of DCM. The latter utilizes a Bayesian approach to define the values of coupling between the sources via fitting of the cross-spectral densities calculated for the DCM-model and the densities, obtained for the original source signals comprised in the tinnitus network.

Bayesian selection of an optimal model for a neural tinnitus network

It is known that model selection is an essential component of any DCM study and cannot be omitted unless there is extremely strong a priori knowledge about the model (Stephan et al., 2010). In our case the hypothesis of interest concerns the estimates of particular parameters in an optimal model of a phantom sound network. For this reason, BMS selection is the first necessary step in a sequential procedure, where inference about particular parameters follows an initial model selection procedure (Stephan et al., 2010).

As described in Sec. 3.2 A model-free approach to the detection of a tinnitus network structure, the information about the structure of the tinnitus network was obtained by means of a model-free approach. We used these preliminary results to build a model space and find the most appropriate model for the DCM. We restricted ourselves to the set of sources, whose strengths of mutual couplings were altered by CR neuromodulation. These sources are located in the left and right primary and secondary auditory cortices as well as in the dorsolateral prefrontal cortex and posterior cingulate cortex. The proposed structure of the neural tinnitus network is also supported by the results of anatomical studies. In accordance to the results of these studies, combining electrophysiological recordings and anatomical tracing, there are pathways originating in auditory fields of the superior temporal region and terminating in distinct regions of the frontal lobes (Romanski et al., 1999a,b). Prefrontal cortex is known to exert inhibitory output to multiple cortical and subcortical regions (Alexander et al., 1976) and has been shown to gate input to primary sensory cortices (Skinner and Yingling, 1977). Furthermore, it was established that the dorsolateral prefrontal cortex exerts early inhibitory modulation of input to primary auditory cortex in humans (Knight et al., 1989). The results of a

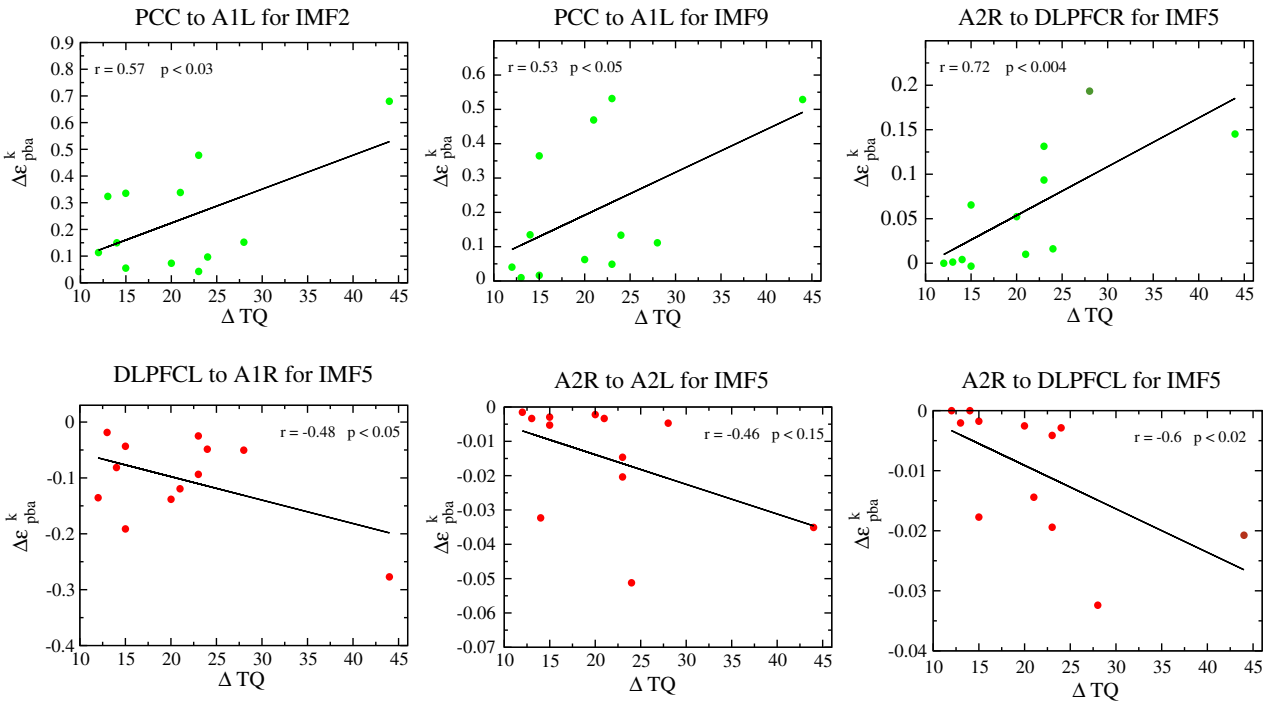

Fig. 5. Changes of effective connectivity in the group of good responders after CR therapy, defined in Eq. (6), as a function of changes in TQ scores. Analysis was performed for those connections, which were significantly altered after CR therapy (see Fig. 4).

PET-study also indicate involvement of a prefrontal-temporal network in tinnitus perception (Mirz et al., 2000). These results motivated us to consider the presence of the inhibitory connections between dorsolateral prefrontal cortex and primary auditory cortex as a necessary element for our DCM model. Another important element, revealed by our preliminary consideration, is the connection of primary auditory cortex and posterior cingulate cortex. Anatomical connections of the auditory cortical areas with the posterior cingulate cortex in the macaque monkey were revealed by means of retrograde and anterograde tracing methods (Yukie, 1995). This fact allowed us to keep such connections in our model. Let us recall that, according to the DCM approach to the modeling of steady-state responses, all sources are modeled as consisting of three interacting neuronal sub-populations, which establish extrinsic connections of different types to each other (Moran et al., 2007, 2009). The types of extrinsic connections differ from each other in dependence on the type of excited neuronal sub-population. As for instance, an incoming connection to a source is considered as inhibitory if it simultaneously excites the sub-populations of inhibitory and excitatory neurons in granular layers. In contrast, if an incoming connection excites only excitatory spiny cells in granular layers then it has to be considered as excitatory (Moran et al., 2009, 2011). Finally, if an incoming connection excites all three sub-populations then it is called mixed or lateral connection (Moran et al., 2007, 2009).

Given the preliminary information about the structure of the tinnitus network and the types of connections, we built a number of possible DCM models, having similar topologies and differing by the directionalities as well as the types of connections among sources. Then, the cross-spectral densities obtained during the simulation and densities of the original source signals were jointly used to optimize parameters of the different competing DCM models. To build a model space, we examined twenty three different models whose choice was restricted by the assumptions about the directed excitatory influence from PCC to A1L as well as about the inhibitory connection from DLPFCL to A1R. Five of such possible models are presented in Fig. 6a. Having defined a model space, we used BMS, which utilizes a free energy as a measure, to find the best model. The free energy is a lower bound on the model evidence and is used for model selection, when testing a series of possible neural architectures using Bayes Factors (Chumbley et al., 2007; Moran et al., 2011). The maximization of the free energy (which bounds log-evidence) ensures a maximum accuracy or data-fit, under complexity constraints. The results of the BMS for the five selected models are presented in Fig. 6b. As seen from the figure, the model 5 strongly outperforms all other models and can be considered as the best one. It is necessary to note here that the models which are drawn in Fig. 6a are the best ones in terms of the free energy estimates and characterized by the minimal complexity (Moran et al., 2007, 2009; Stephan et al., 2010). The best model includes a bidirectional lateral coupling between left and right primary auditory cortices along with the other connections, which are similar to the preliminary connections detected in A model-free approach to the detection of a tinnitus network structure.

Alteration of effective connectivity by CR neuromodulation: the results of DCM

Based on the observation of a qualitative transformation of the spectral characteristics in the group of good responders due to CR treatment and assuming stationarity in our recordings, we characterized their steady-state behavior before and after CR treatment using cross spectral densities (Moran et al., 2009, 2011). Given the optimal structure of the model 5 and using the cross spectral densities, we inverted the DCM models for each control subject and each patient from the group of good responders before and after CR treatment. Model inversion entails estimating the mean and variance of the unknown model parameters that summaries their posterior or conditional density. These unknown parameters include the biophysical parameters of the neural-mass model as well as parameters controlling the spectral composition of neuronal and channel noise. These noise parameters control a mixture of white and pink noise and are assumed to exist at all brain areas separately. The priors on these unknown parameters used standard values (Moran et al., 2009).

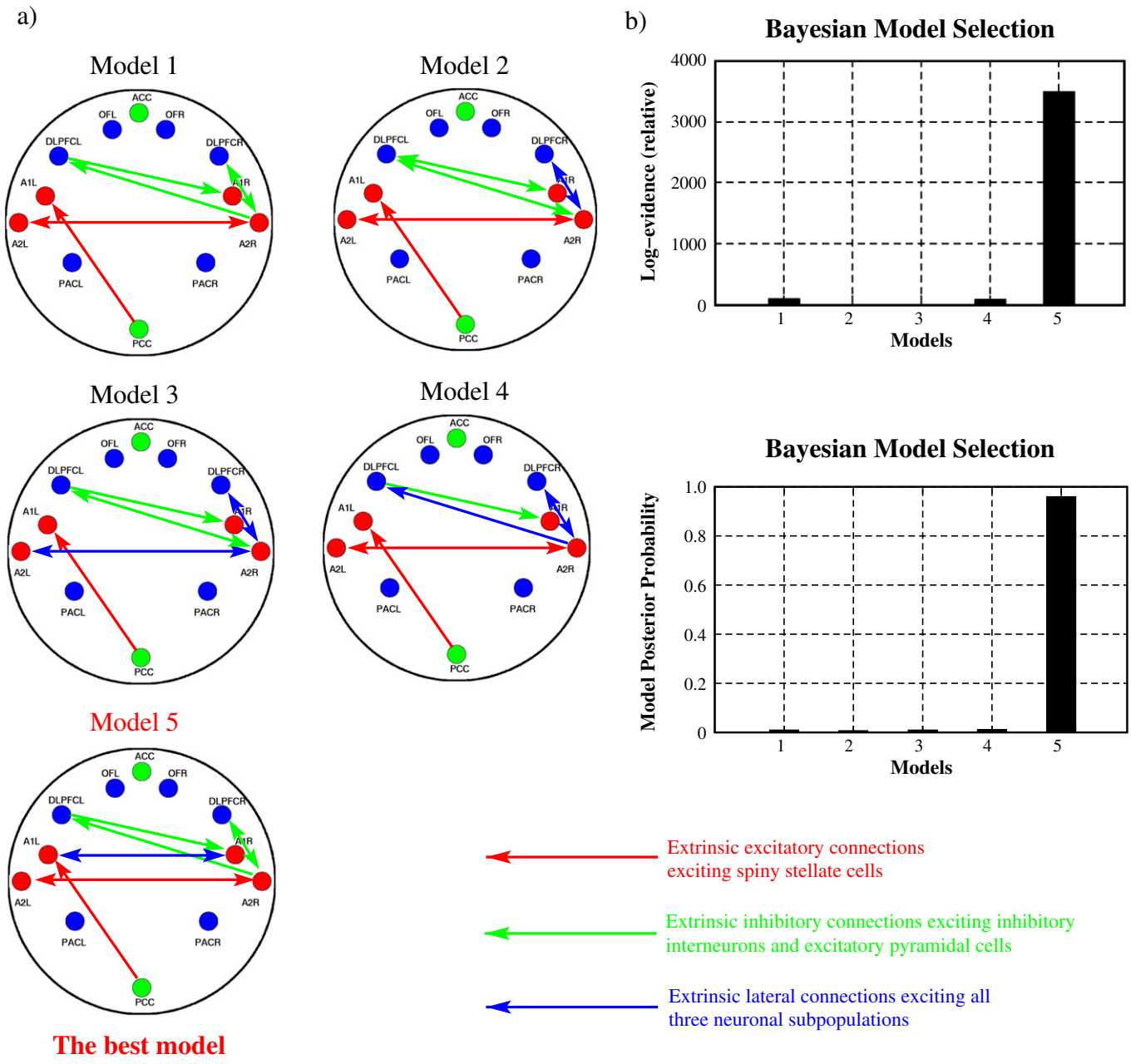

Fig. 6. a) Schematic presentation of the five different DCM models chosen for BMS. Different types of coupling between sources in the models are represented by the arrows of three different colors. The presence of arrows on both ends stands for a bidirectional coupling of the same type for each direction. b) The histograms containing the estimates of the free energy for the models pictured in a) and their posterior probabilities.

The observed and modeled magnitudes of the cross spectral densities, averaged over subjects in the control group and in the group of good responders before and after CR treatment, are presented in Fig. 7. Clearly, the DCMs reproduce the key spectral properties of the source signals in both groups as well as the their transformation induced by the CR neuromodulation. Indeed, the cross-spectra from the control group contain a very pronounced alpha peak and relatively low power at the frequencies below 10 Hz as captured by the control DCMs. On the other hand, the source signals of the tinnitus patients before CR treatment were characterized by an increased low-frequency power and decreased amplitude of the alpha oscillations, what was also shown by the tinnitus DCMs. The DCMs of the tinnitus patients after CR treatment demonstrate the reduction of the low-frequency activity and the restoration of alpha power to the control values. The observed high sensitivity of the DCM to the changes in alpha oscillations may be partly explained by the fact that the original model of a cortical column was designed to reproduce alpha rhythm (Jansen and Rit, 1995). It is necessary to note here, that for the sake of presentation clarity, the frequency range for the cross-spectral densities shown in Fig. 7 was restricted to values from 1 to 40 Hz. The behavior of the cross-spectral densities in the gamma frequency band, being examined for the tinnitus patients before and after CR treatment, agree well with the above results for the power spectra. In particular, the oscillatory response of the tinnitus network in the gamma band was significantly altered by CR neuromodulation in the group of good responders, which is illustrated below by the changes in a shape of the averaged transfer function presented in Fig. 8b.

The *maximum a posteriori* (MAP) estimates of the connection strengths were calculated via averaging over individual estimates for the control group as well as for the group of good responders

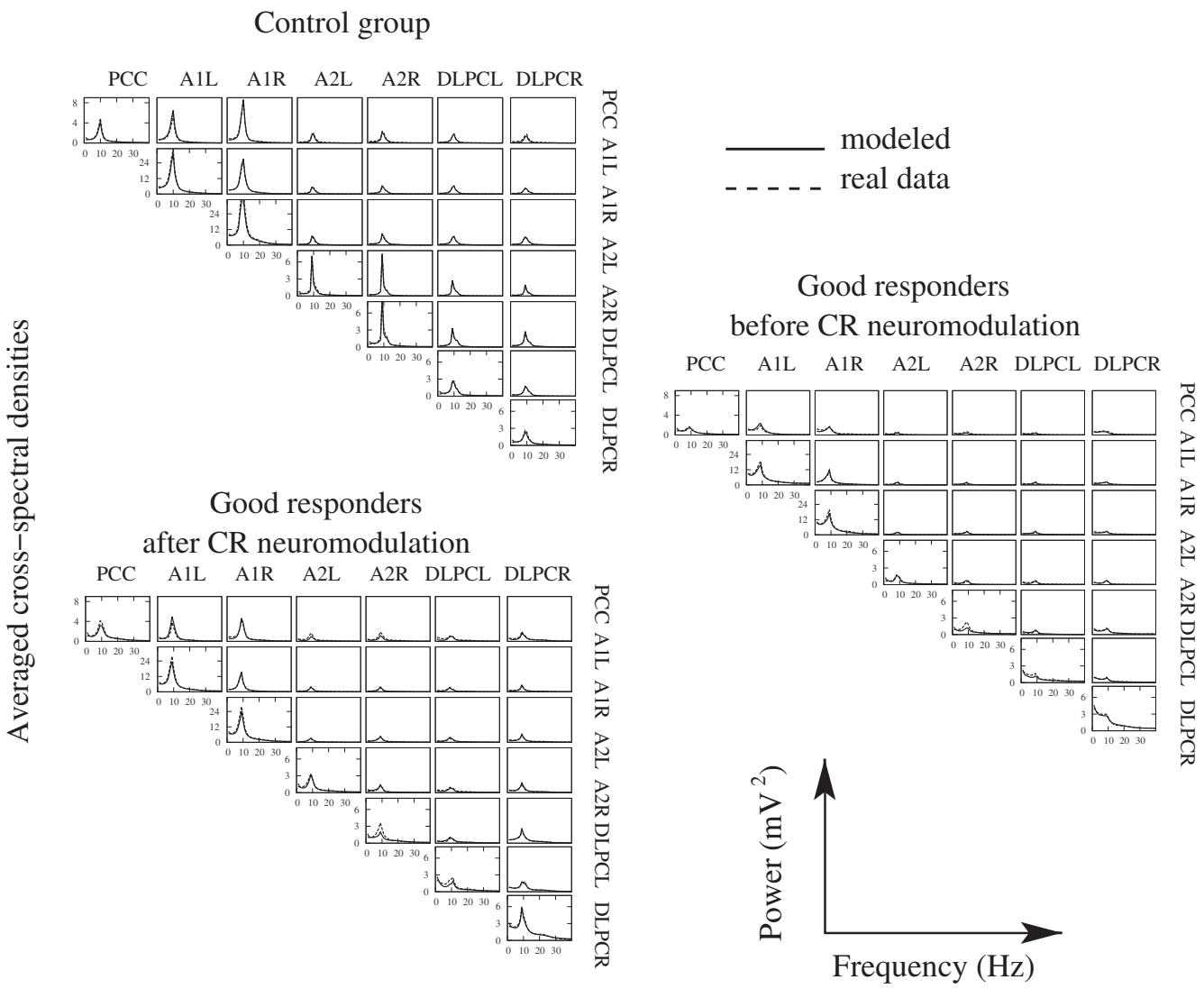

Fig. 7. Observed and modeled averaged cross-spectral densities. The individual cross-spectral densities were calculated for frequencies from 1 to 90 Hz by using a vector autoregressive model. The averaged cross-spectral densities for the source signals (dashed lines) included in model 5 and the averaged DCM fits (solid lines) are both presented for the healthy controls and for the tinnitus patients before and after CR therapy. The main diagonal contains of spectral densities at each source included in the model, while the off-diagonal elements display the two-way cross spectra. Here, for the sake of clarity, we illustrate changes in cross-spectral densities in the range from 1 to 40 Hz only (see text for details).

before and after CR neuromodulation. Then, the control MAP estimates and estimates for the good responders before and after CR treatment were sequentially compared via one-way ANOVA corrected for multiple comparisons (Hochberg and Tamhane, 1987). Mean values of MAP estimates for the control group and for the group of good responders before and after CR treatment are plotted in Fig. 8a together with 95% confidence intervals. As follows from the presented results, the connection of PCC and A1L in good responders before CR treatment was significantly stronger than in the control group. The strength of this connection was significantly altered by CR neuromodulation and after CR therapy became indistinguishable from the control values. According to the classification used in Bayesian selection of an optimal model for a neural tinnitus network, this was an excitatory connection exciting a subpopulation of spiny stellate cells. In addition, CR neuromodulation significantly changes the strength of the connection of DLPCFL and A1R. That connection was of inhibitory type and was weakened in the tinnitus patients, as illustrated in Fig. 8a by the presence of corresponding statistically significant difference of the control and tinnitus MAPs. CR neuromodulation caused a drastic increase of inhibitory driving from DLPCFL to A1R. Another inhibitory connection, which was pathologically strengthened in our tinnitus patients, is the connection between DLPFCR and A2R. CR therapy significantly alters the strength of this connection, making it indistinguishable from the control values. The excitatory connections between left and right secondary auditory cortices were significantly altered in asymmetric manner from A2L to A2R. Finally, the lateral connection between left and right primary auditory cortices was significantly weakened by CR therapy. This might be caused by the fact that low-frequency oscillatory activity in the delta band was strongly reduced due to the desynchronizing effect of CR neuromodulation and, probably, reflects its long-lasting, relearning effect on the dynamics of neural networks (Tass et al., 2009, 2012a,b).

The DCM for the steady-state responses utilizes a spectral formulation of neural mass models when it is assumed that sources of EEG activity apply a filter-like operation to their inputs so that the input frequencies are modulated by its transfer function. Moreover, in linear systems analysis, the Laplace transform allows one to formulate the system's time domain equations of motion in terms of frequency domain operators that are characterized by the system's transfer function (Moran et al., 2008). Accordingly, in the case of a few interacting sources their individual transfer functions may be

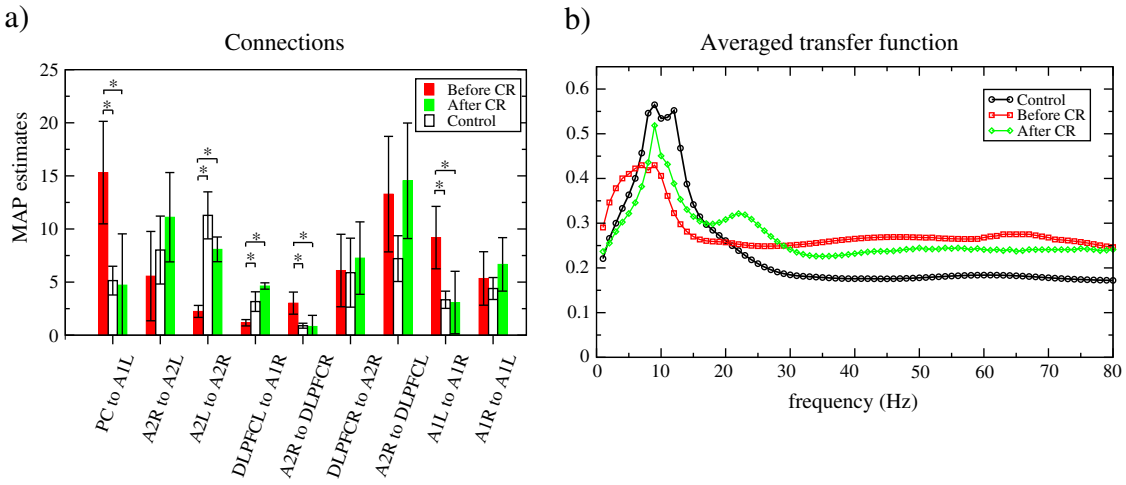

Fig. 8. a) Mean values of the MAP estimates of extrinsic connectivity parameters in the control group and in the group of good responders before and after CR treatment. Connections with a significantly (with $p < 0.05$) different strength compared to the control values are labeled by asterisks. Connections for which the MAP estimates were significantly altered by CR neuromodulation are also labeled by asterisks. b) The partial transfer functions defined as the ratio the off-diagonal averaged cross-spectral densities in Fig. 7 and the corresponding diagonal averaged auto-spectral densities of the source signals were averaged over all sources to get the averaged transfer function. Calculations were performed for the averaged cross-spectral densities obtained both for the healthy controls and for the good responders before and after CR treatment.

defined as ratios of the source-target cross spectral densities and corresponding auto-spectral densities of the sources. To calculate the normalized partial transfer functions for the cross spectral densities averaged over groups of patients or control subjects, we divided the off-diagonal cross spectral densities shown in Fig. 7 by the corresponding diagonal auto-spectral densities. Then, we averaged all normalized partial transfer functions over all sources to characterize the transformation of the spectral response of the neural tinnitus network as a whole. The results of our calculations are presented in Fig. 8b. In the case of the control group the averaged normalized transfer function has one large peak at 10 Hz which corresponds to the presence of the auditory alpha rhythm in the studied network. This result means that in a "healthy" state the network structure is organized in such a way that it amplifies oscillatory input activity in the alpha band and suppresses all oscillations in the delta and gamma bands. The averaged transfer function calculated for the group of good responders before CR treatment has two maxima one of which is located at high frequencies and related to the enhanced gamma activity, whereas another one is shifted to lower frequencies and corresponds to the enhanced activity in the delta band. At the same time, the alpha peak is strongly reduced in comparison with the similar peak of the control group. The averaged normalized transfer function nicely describes the qualitative transformation of the spectral response of the tinnitus network to a "pathological" state, when the strengths of connections between network elements are upregulated in such a way that input activity is enhanced in the gamma and delta bands and drastically attenuated in the alpha band. As can further be seen from the Fig. 8b, the acoustic CR therapy results in a restoration of the alpha peak together with a complete elimination of the peaks in the gamma and delta frequency bands. The presence of a small peak in the beta band may be explained by the absence of any significant changes in this band caused by CR stimulation. As we already mentioned in Changes in oscillatory activity induced by CR neuromodulation, the beta power was found to be higher of the control values in some regions of interest related to the emotional side of the sound processing. This kind of activity was not perturbed by CR neuromodulation and manifested itself as a small peak after averaging over the cross spectral densities of all sources.

Discussion

We here studied changes in oscillatory power and effective connectivity in the group of good responders before and after CR neuromodulation as well as in the group of healthy controls. Overall, our results show that the CR therapy significantly normalized both power and causal interactions within a tinnitus-related network. In particular, we found statistically significant CR-induced power changes, i.e. a decrease of delta and gamma along with a substantial increase of alpha, in A1, DLPFC and PCC. In a previous study, CR-induced power changes of the same EEG data were analyzed by means of sLORETA and conventional bandpass filtering (Tass et al., 2012a). The results in that study were in a good agreement with our results presented here, except for the fact that in the previous study in PCC no significant CR-induced power changes were detected in the gamma band. The approach, used in the present study, might be more sensitive due to the adaptive filtering via EMD, which allows to avoid drawbacks caused by edge effects (Silchenko et al., 2010).

Interestingly, a characteristic structure of the power spectra in the case of tinnitus is a similar one to that observed during the successful retrieval of complex semantic structures from memory (Klimesch et al., 1997). Accordingly, one may speculate that tinnitus is a persistent attempt of the brain to recall and classify some aberrant sounds pulled from memory. In accordance with recent experimental findings, chronic subjective tinnitus is characterized by the simultaneous alteration of brain activity in prefrontal cortex and posterior cingulate cortex together with weakening of auditory alpha-like rhythmic activity (Lorenz et al., 2009; Weisz et al., 2011). The absence of the therapeutic effect in the case of non-responders correlated with the absence of any significant changes in the alpha band and remained enhanced oscillatory activity in gamma and delta frequency bands, which is still observed in temporal areas and posterior cingulate cortex. In particular, the fact that alpha rhythm was not affected by CR neuromodulation might indicate that excitatory–inhibitory disbalance, which is thought to be related to this rhythm (Weisz et al., 2011), was not restored in this case.

Moreover, in tinnitus patients before CR therapy we revealed an increased strength of the interaction between the A1 and PCC. The latter is known to be involved in cognitive aspects of auditory processing (Laufer et al., 2009). Indeed, the PCC is supposed to exert a silence based cognitive auditory comparator function (Laufer et al., 2009). In the case of tinnitus distress, when the PCC is not able to exert its salience based comparator function, an aberrant auditory sound might penetrate from hippocampal memory (De Ridder et al., 2006; Vanneste et al., 2010, 2011) via dysfunctional parahippocampal sensory gating (Boutros et al., 2008; Vanneste et al., 2012). The persistent attempts to recall and classify an aberrant sound might lead to sustained pathological neuronal synchrony in the primary auditory

cortex and a paradoxical auditory memory for tinnitus which is considered to be the initial process in the transition of the sensory to the affect component (Shulman, 1995). Thus, the activity in the PCC might be linked to a successful retrieval from auditory memory (Klimesch, 2012; Klimesch et al., 1997; Sadaghiani et al., 2009; Shannon and Buckner, 2004), which is accompanied by an increase of theta power and a significant reduction in alpha power (Klimesch et al., 1997). The latter observation is in line with recent findings concerning a possible role of the alpha rhythm in cognition and functional inhibition (Hartmann et al., 2012; Jensen and Mazaheri, 2010; Klimesch, 2012; Klimesch et al., 2007; Weisz et al., 2011). Indeed, the power of the auditory alpha rhythm reflects the state of excitatory–inhibitory balance and tends to decrease in the aftermath of a word or other linguistic stimulus presentation (Klimesch, 1997; Klimesch et al., 1997). Moreover, the expectancy of aversive auditory feedback modulates perception of sounds and these fluctuating perceptions become manifest in a modulation of stimulus-induced desynchronization of the alpha rhythm (Hartmann et al., 2012). The reported sensitivity of the auditory alpha rhythm to aversive auditory feedback might mean the involvement in auditory processing of non-auditory brain areas responsible for short-time memory and attention.

Furthermore, we found a deficiency of inhibitory interaction in the alpha band between the dorsolateral prefrontal cortex and the primary auditory cortex. This result is in line with recent experimental findings, concerning the alterations of gamma aminobutyric acid (GABA) neuronal function and benzodiazepine receptor (BZR) function, which were found to be implicated in the pathophysiology of severe, chronic tinnitus (Daftary et al., 2004; Shulman and Goldstein, 2006, Shulman and Goldstein, 2009). The evaluation of the density of the BZR is used in studies on the role of GABA mechanisms in neuropsychiatric disorders (Bremner et al., 2000). The decrease in BZR binding is associated with the reduced receptor affinity resulting in a deficiency of GABAergic transmission. The single-photon emission computed tomography (SPECT) imaging in patients with severe, intractable central tinnitus showed a significant reduction of the BZR density in the left frontal lobe which means a possible impairment of GABA-A receptors assisted inhibitory transmission in non-auditory areas (Daftary et al., 2004). Thus, the deficiency in GABAergic transmission in temporal and frontal areas is commonly observed in the cases of severe intractable tinnitus (Daftary et al., 2004; Shulman, 1995) and might be the reason for a reduced inhibition in our case as well. It was also hypothesized that a fundamental function of the amygdala-hippocampal structures might be the establishment of such an alteration in auditory masking which was found in all tinnitus patients (Shulman, 1995). The mechanisms underlying a paradoxical auditory memory for tinnitus are hypothesized to be characterized by a diminution of inhibition mediated by GABA-A receptors due to a disconnection from excitatory (glutamate) inputs (Shulman, 1995). These findings are in line with our results reported above in Alteration of effective connectivity by CR neuromodulation: the results of DCM Sec. 3.4, concerning the diminution of inhibitory coupling between primary auditory cortex and dorsolateral prefrontal cortex in tinnitus patients before CR stimulation.

Thus, the results of DCM, considered together with the results of our connectivity analysis, show that the good responders prior to CR therapy are characterized by an excessive excitatory coupling between PCC and A1, as opposed to healthy controls. In addition, prior to CR therapy inhibitory connections between DLPFC and A1 were significantly weaker in good responders compared to healthy controls. Remarkably, in the good responders 12 weeks of CR therapy eliminated nearly all pathological connections within the tinnitus network comprising auditory and non-auditory areas. In fact, by reversing the strength of excitatory and inhibitory connections, CR therapy specifically counteracted the excitatory–inhibitory disbalance, observed prior to CR treatment, and makes the difference in effective connectivity between good responders and healthy controls statistically insignificant. Moreover, CR therapy qualitatively changes the spectra response of the tinnitus network by modifying the shape of the averaged transfer function, so that the latter becomes similar to that one observed for the control group.

Our findings fit nicely to the recently proposed model framework directly relating synchronization in auditory regions and loss of inhibition (Lorenz et al., 2009; Weisz et al., 2007b, 2011). According to this framework, a reduced afferent input in frequency regions affected by a peripheral damage leads to an overall reduced neuronal activity within the deprived region, equally affecting excitatory as well as inhibitory neurons. It was proposed that in a circumscribed region of tonotopically organized auditory fields, downregulation of inhibitory drive is strong enough and excitatory neurons are not hyperpolarized sufficiently, that the latter spontaneously synchronize their activity (Weisz et al., 2011). Indeed, it might be that a combined action of deafferentation, weakening inhibition, and persistent recalls from the limbic system, increasing the rate of spontaneous activity in a circumscribed region of the primary auditory cortex, underlies the emergence of pathological synchrony and tinnitus perception.

As follows from our results, chronic tinnitus is characterized by a strong imbalance of excitation and inhibition. Moreover, a statistically significant improvement in TQ and VAS scores for the group of good responders (Tass et al., 2012a), is accompanied by restoration of the excitatory–inhibitory balance after CR neuromodulation and qualitative changes of effective connectivity within the tinnitus neuronal network.

Appendix A. Supplementary data

Supplementary data to this article can be found online at http://dx.doi.org/10.1016/j.neuroimage.2013.03.013.

References

Adamchic, I., Hauptmann, C., Tass, P.A., 2012a. Changes of oscillatory activity in pitch processing network and related tinnitus relief induced by acoustic CR neuromodulation. Front. Neurosci. 6. http://dx.doi.org/10.3389/fnsys.2012.00018.

Adamchic, I., Tass, P.A., Langguth, B., Hauptmann, C., Koller, M., Schecklmann, M., Zeman, F., Landgrebe, M., 2012b. Linking the Tinnitus Questionnaire and the subjective Clinical Global Impression: Which differences are clinically important? Health Qual. Life Outcomes 10. http://dx.doi.org/10.1186/1477-7525-10-79.

Adamchic, I., Langguth, B., Hauptmann, C., Tass, P.A., 2012c. Psychometric evaluation of Visual Analog Scale for the assessment of chronic tinnitus. Am. J. Audiol. 10. http://dx.doi.org/10.1044/1059-0889(2012/12-0010.

Alain, C., Woods, D.L., Knight, R.T., 1998. A distributed cortical network for auditory sensory memory in humans. Responses to aversive visual stimuli. Brain Res. 812, 2337.

Alexander, G.E., Newman, J.D., Symmes, D., 1976. Convergence of prefrontal and acoustic inputs upon neurons in the superior temporal gyfus of the awake squirrel monkey. Brain Res. 116, 334–338.

Axelsson, A., Prasher, D., 2000. Tinnitus induced by occupational and leisure noise. Noise Health 2, 47–54.

Baccala, L.A., Sameshima, K., 2001. Partial directed coherence: a new concept in neural structure determination. Biol. Cybern. 84, 463–474.

Bendor, D., Wang, X.Q., 2005. The neuronal representation of pitch in primate auditory cortex. Nature 436, 1161–1165.

Bledowski, C., Kadosh, K.C., Wibral, M., Rahm, B., Bittner, R.A., Hoechstetter, K., Scherg, M., Maurer, K., Goebel, R., Linden, D.E.J., 2012. Mental chronometry of working memory retrieval: a combined functional magnetic resonance imaging and event-related potentials approach. J. Neurosci. 26. http://dx.doi.org/10.1523/JNEUROSCI.3542-05.2006.

Boggio, et al., 2008. Modulatory effects of anodal transcranial direct current stimulation on perception and pain thresholds in healthy volunteers. Eur. J. Neurol. 15, 1124–1130.

Boutros, N.N., Mears, R., Pflieger, M.E., Moxon, K.A., Ludowig, E., Rosburg, T., 2008. Sensory gating in the human hippocampal and rhinal regions: regional differences. Hippocampus 18, 310–316.

Bremner, J.D., Innis, R.B., Southwick, S.M., Staib, L., Zoghbi, S., Charney, D.S., 2000. Decreased benzodiazepine receptor binding in prefrontal cortex in combat-related posttraumatic stress disorder. Am. J. Psychiatry 157, 1120–1126.

Chittka, L., Brockmann, A., 2005. Perception space — the final frontier. PLoS Biol. 4, 564–568.

Chumbley, J., Friston, K., Fearn, T., Kiebel, S., 2007. A Metropolis–Hastings algorithm for dynamic causal models. Neuroimage 38, 478–487.

Daftary, A., Shulman, A., Strashun, A.M., Gottschalk, C., Zoghbi, S.S., Seiby, J.P., 2004. Benzodiazepine receptor distribution in severe intractable tinnitus. Int. Tinnitus J. 10, 17–23.

De Ridder, D., Fransen, H., Francois, O., Sunaert, S., Kovacs, S., van de Heyning, P., 2006. Amygdalohippocampal involvement in tinnitus and auditory memory. Acta Otolaryngol. Suppl. 50–53.
De Ridder, D., Van Der Loo, E., Vanneste, S., Gais, S., Plazier, M., Kovacs, S., Sunaert, S., Menovsky, T., Van De Heyning, P., 2011. Theta–gamma dysrhythmia and auditory phantom perception. J. Neurosurg. 114, 912–921.
Dohrmann, K., Weisz, N., Schlee, W., Hartmann, T., Elbert, T., 2007. Neurofeedback for treating tinnitus. Prog. Brain Res. 166, 473–554.
Eggermont, J.J., Roberts, L.E., 2004. The neuroscience of tinnitus. Trends Neurosci. 27, 676–682.
Engineer, N.D., Riley, J.R., Seale, J.D., Vrana, W.A., Shetake, J.A., Sudanagunta, S.P., Borland, M.S., Kilgard, M.P., 2011. Reversing pathological neural activity using targeted plasticity. Nature 470, 101–104.
Florin, E., Gross, J., Pfeifer, J., Fink, G.R., Timmermann, L., 2010. The effect of filtering on Granger causality based multivariate causality measures. Neuroimage 50, 577–588.
Fregni, F., et al., 2006. Treatment of major depression with transcranial direct current stimulation. Bipolar Disord. 8, 203–204.
Hall, D.A., Lainez, M.J.A., Newman, C.W., Sanchez, T.G., Egler, M., Tennigkeit, F., Koch, M., Langguth, B., 2012. Treatment options for subjective tinnitus: self reports from a sample of general practitioners and ENT physicians within Europe and the USA. BMC Health Serv. Res. 11, 302–316.
Hartmann, T., Schlee, W., Weisz, N., 2012. It's only in your head: expectancy of aversive auditory stimulation modulates stimulus-induced auditory cortical alpha desynchronization. Neuroimage 60, 170–178.
Hauptmann, C., Tass, P.A., 2009. Cumulative and after-effects of short and weak coordinated reset stimulation: a modeling study. J. Neural Eng. 6, 016004.
Hochberg, Y., Tamhane, A.C., 1987. Multiple Comparison Procedures. John Wiley and Sons, Hoboken, NJ.
Huang, N.E., Shen, Z., Long, S.R., Wu, M.L.C., Shih, H.H., Zheng, Q.N., Yen, N.C., Tung, C.C., Liu, H.H., 1998. The empirical mode decomposition and the Hilbert spectrum for nonlinear and non-stationary time series analysis. Proc. R. Soc. A Math. Phys. Eng. Sci. 454, 903–995.
Jacobson, N.S., Truax, P., 1991. Clinical significance: a statistical approach to defining meaningful change in psychotherapy research. J. Consult. Clin. Psychol. 59, 12–19.
Jansen, B.H., Rit, G.R., 1995. Electroencephalogram and visual evoked potential generation in a mathematical model of coupled cortical columns. Biol. Cybern. 73, 357–366.
Jensen, O., Mazaheri, A., 2010. Shaping functional architecture by oscillatory alpha activity: gating by inhibition. Front. Hum. Neurosci. 4, 1–8.
Kahlbrock, N., Weisz, N., 2008. Transient reduction of tinnitus intensity is marked by concomitant reductions of delta band power. BMC Biol. 6, 4. http://dx.doi.org/10.1186/1741-7007-6-4.
Klimesch, W., 1997. EEG-alpha rhythms and memory processes. Int. J. Psychophysiol. 26, 319–340.
Klimesch, W., 2012. Alpha-band oscillations, attention, and controlled access to stored information. Trends Cogn. Sci. 16, 606–617.
Klimesch, W., Doppelmayr, M., Schimke, H., Ripper, B., 1997. Theta synchronization and alpha desynchronization in a memory task. Psychophysiology 34, 169–176.
Klimesch, W., Sauseng, P., Hanslmayr, S., 2007. EEG alpha oscillations: the inhibition-timing hypothesis. Brain Res. Rev. 53, 63–88.
Knight, R.T., Scabini, D., Woods, D.L., 1989. Prefrontal cortex gating of auditory transmission in humans. Brain Res. 504, 338–342.
Langers, D.R.M., de Kleine, E., van Dijk, P., 2012. Tinnitus does not require macroscopic tonotopic map reorganization. Front. Syst. Neurosci. 6, 2. http://dx.doi.org/10.3389/fnsys.2012.00002.
Lanting, C.P., de Kleine, E., van Dijk, P., 2009. Neural activity underlying tinnitus generation: results from PET and fMRI. Hear. Res. 255, 1–13.
Laufer, I., Negishi, M., Constable, R.T., 2009. Comparator and non-comparator mechanisms of change detection in the context of speech and ERP study. Neuroimage 44, 546–562.
Leaver, A.M., Renier, L., Chevillet, M.A., Morgan, S., Kim, H.J., Rauschecker, J.P., 2011. Dysregulation of limbic and auditory networks in tinnitus. Neuron 69, 33–43.
Lewis, J.W., Beauchamp, M.S., DeYoe, E.A., 2000. A comparison of visual and auditory motion processing in human cerebral cortex. Cereb. Cortex 10, 873–888.
Llinas, R.R., Ribary, U., Jeanmonod, D., Kronberg, E., Mitra, P.P., 1999. Thalamocortical dysrhythmia: a neurological and neuropsychiatric syndrome characterized by magnetoencephalography. Proc. Natl. Acad. Sci. U. S. A. 96, 15222–15227.
Lorenz, I., Mueller, N., Schlee, W., Hartmann, T., Weisz, N., 2009. Loss of alpha power is related to increased gamma synchronization — a marker of reduced inhibition in tinnitus? Neurosci. Lett. 453, 225–228.
Lysyansky, B., Popoych, O.V., Tass, P.A., 2011. Desynchronizing anti-resonance effect of *m*:*n* ON–OFF coordinated reset stimulation. J. Neural Eng. 8, 036019.
Mirz, F., Gjedde, A., Ishizu, K., Pedersen, C.B., 2000. Cortical networks subserving the perception of tinnitusa PET study. Acta Otolaryngol. Suppl. 543, 241–243.
Mitchell, T.V., et al., 2005. Functional magnetic resonance imaging measure of automatic and controlled auditory processing. Neuroreport 16, 457–461.
Moran, R.J., Kiebel, S.J., Stephan, K.E., Reilly, R.B., Daunizeau, J., Friston, K.J., 2007. A neural mass model of spectral responses in electrophysiology. Neuroimage 37, 706–720.
Moran, R.J., Stephan, K.E., Kiebel, S.J., Rombach, N., O'Connor, W.T., Murphy, K.J., Reilly, R.B., Friston, K.J., 2008. Bayesian estimation of synaptic physiology from the spectral responses of neural masses. Neuroimage 42, 272–284.
Moran, R.J., Stephan, K.E., Seidenbecher, T., Pape, H.-C., Dolan, R.J., Friston, K.J., 2009. Dynamic causal models of steady-state responses. Neuroimage 44, 796–811.
Moran, R.J., Mallet, N., Litvak, V., Dolan, R.J., Magill, P.J., Friston, K.J., Brown, P., 2011. Alterations in brain connectivity underlying beta oscillations in Parkinsonism. PLoS Comput. Biol. 7, e1002124.
Muhlnickel, W., Elbert, T., Taub, E., Flor, H., 1998. Reorganization of auditory cortex in tinnitus. Proc. Natl. Acad. Sci. U. S. A. 95, 10340–10343.
Neiman, A.B., Russell, D.F., Yakusheva, T.A., Dilullo, A., Tass, P.A., 2007. Response clustering in transient stochastic synchronization and desynchronization of coupled neuronal bursters. Phys. Rev. E 76, 021908.
Norena, A.J., Eggermont, J.J., 2003. Changes in spontaneous neural activity immediately after an acoustic trauma: implications for neural correlates of tinnitus. Hear. Res. 183, 137–153.
Norena, A., Micheyl, C., Chery-Croze, S., Collet, L., 2002. Psychoacoustic characterization of the tinnitus spectrum: implications for the underlying mechanisms of tinnitus. Audiol. Neurootol. 7, 358–369.
Ochi, K., Eggermont, J.J., 1997. Effects of quinine on neural activity in cat primary auditory cortex. Hear. Res. 105, 105–118.
Popovych, O.V., Tass, P.A., 2012. Desynchronizing electrical and sensory coordinated reset neuromodulation. Front. Hum. Neurosci. 6. http://dx.doi.org/10.3389/fnhum.2012.00058.
Rauschecker, J.P., Leaver, A.M., Muehlau, M., 2010. Tuning out the noise: limbic–auditory interactions in tinnitus. Neuron 66, 819–826.
Rilling, B., Flandrin, P., Gonvalves, P., 2003. On empirical mode decomposition and its algorithms. IEEE-EURASIP Workshop on Nonlinear Signal and Image Processing NSIP-03, Grado (I).
Rilling, G., Flandrin, P., Goncalves, P., Lilly, J., 2007. Bivariate empirical mode decomposition. IEEE Signal Process. Lett. 14, 936–939.
Robertson, D., Irvine, D.R.F., 1989. Plasticity of frequency organization in auditory cortex of Guinea-pigs with partial unilateral deafness. J. Comp. Neurol. 282, 456–471.
Romanski, L.M., Bates, J.F., Goldman-Rakic, P.S., 1999a. Auditory belt and parabelt projections to the prefrontal cortex in the rhesus monkey. J. Comp. Neurol. 403, 141–157.
Romanski, L.M., Tian, B., Fritz, J., Mishkin, M., Goldman-Rakic, P.S., Rauschecker, J.P., 1999b. Dual streams of auditory afferents target multiple domains in the primate prefrontal cortex. Nat. Neurosci. 2, 1131–1136.
Sadaghiani, S., Hesselmann, G., Kleinschmidt, A., 2009. Distributed and antagonistic contributions of ongoing activity fluctuations to auditory stimulus detection. J. Neurosci. 29, 13410–13417.
Sameshima, K., Baccala, L.A., 1999. Using partial directed coherence to describe neuronal ensemble interactions. J. Neurosci. Methods 94, 93–103.
Schaette, R., McAlpine, D., 2011. Tinnitus with a normal audiogram: physiological evidence for hidden hearing loss and computational model. J. Neurosci. 31, 13452–13457.
Schaette, R., König, O., Hornig, D., Gross, M., Kempter, R., 2010. Acoustic stimulation treatments against tinnitus could be most effective when tinnitus pitch is within the stimulated frequency range. Hear. Res. 269, 95–101.
Schelter, B., Winterhalder, M., Eichler, M., Peifer, M., Hellwig, B., Guschlbauer, B., Lucking, C.H., Dahlhaus, R., Timmer, J., 2005. Testing for directed influences among neural signals using partial directed coherence. J. Neurosci. Methods 152, 210–219.
Schelter, B., Timmer, J., Eichler, M., 2009. Assessing the strength of directed influences among neural signals using renormalized partial directed coherence. J. Neurosci. Methods 179, 121–130.
Scherg, M., Ille, N., Bornfleth, H., Berg, P., 2002. Advanced tools for digital EEG review: virtual source montages, whole-head mapping, correlation, and phase analysis. J. Clin. Neurophysiol. 19, 91–112.
Schlee, W., Mueller, N., Hartmann, T., Keil, J., Lorenz, I., Weisz, N., 2009a. Mapping cortical hubs in tinnitus. BMC Biol. 7, 80.
Schlee, W., Hartmann, T., Langguth, B., Weisz, N., 2009b. Abnormal resting-state cortical coupling in chronic tinnitus. BMC Neurosci. 10, 11.
Schlogl, A., 2006. A comparison of multivariate autoregressive estimators. Signal Process. 86, 2426–2429.
Shannon, B.J., Buckner, R.L., 2004. Functional-anatomic correlates of memory retrieval that suggest nontraditional processing roles for multiple distinct regions within posterior parietal cortex. J. Neurosci. 24, 10084–10092.
Shulman, A., 1995. A final common pathway for tinnitus — the medial temporal lobe system. Int. Tinnitus J. 1, 115–126.
Shulman, A., Goldstein, B., 2006. Pharmacotherapy for severe, disabling, subjective, idiopathic tinnitus: 2005–2006. Int. Tinnitus J. 12, 161–171.
Shulman, A., Goldstein, B., 2009. Subjective idiopathic tinnitus and palliative care: a plan for diagnosis and treatment. Otolaryngol. Clin. N. Am. 42, 15–37.
Silchenko, A.N., Adamchic, I., Pawelczyk, N., Hauptmann, C., Maarouf, M., Sturm, V., Tass, P., 2010. Data-driven approach to the estimation of connectivity and time delays in the coupling of interacting neuronal subsystems. J. Neurosci. Methods 191, 32–44.
Skinner, J.E., Yingling, C.D., 1977. Central gating mechanisms that regulate event-related potentials and behavior. Attention, Voluntary Contraction and Event-Related Cerebral Potentials. Progress in Clinical Neurophysiology, 1. Karger, Basel, pp. 30–69.
Stephan, K.E., Penny, W.D., Daunizeau, J., Moran, R.J., Friston, K.J., 2009. Bayesian model selection for group studies. Neuroimage 46, 1004–1017.
Stephan, K.E., Penny, W.D., Moran, R.J., den Ouden, H.E.M., Daunizeau, J., Friston, K.J., 2010. Ten simple rules for dynamic causal modeling. Neuroimage 49, 3099–3109.
Strand, N.A., 1977. Multichannel complex maximum entropy (autoregressive) spectral analysis. IEEE Trans. Autom. Control 22, 634–640.
Takahashi, D.Y., Baccala, L.A., Sameshima, K., 2007. Connectivity inference between neural structures via partial directed coherence. J. Appl. Stat. 34, 1259–1273.
Tass, P.A., 1999. Phase resetting in medicine and biology: stochastic modelling and data analysis. Springer-Verlag, Berlin.
Tass, P.A., 2003a. Desynchronization by means of a coordinated reset of neural subpopulations — a novel technique for demand-controlled deep brain stimulation. Prog. Theor. Phys. Suppl. 150, 281–296.

Tass, P.A., 2003b. A model of desynchronizing deep brain stimulation with a demand-controlled coordinated reset of neural subpopulations. Biol. Cybern. 89, 81–88.
Tass, P.A., Hauptmann, C., 2009. Anti-kindling achieved by stimulation targeting slow synaptic dynamics. Restor. Neurol. Neurosci. 27, 589–609.
Tass, P.A., Majtanik, M., 2006. Long-term anti-kindling effects of desynchronizing brain stimulation: a theoretical study. Biol. Cybern. 94, 58–66.
Tass, P.A., Popovych, O.V., 2012. Unlearning tinnitus-related cerebral synchrony with acoustic coordinated reset stimulation — theoretical concept and modelling. Biol. Cybern. 106, 27–36.
Tass, P.A., Silchenko, A.N., Barnikol, U., Hauptmann, C., Speckmann, E.J., 2009. Long-lasting desynchronization in rat hippocampal slice induced by coordinated reset stimulation. Phys. Rev. E 80. http://dx.doi.org/10.1103/PhysRevE.80.011902.
Tass, P.A., Adamchic, I., Freund, H.J., von Stackelberg, T., Hauptmann, C., 2012a. Counteracting tinnitus by acoustic coordinated reset neuromodulation. Restor. Neurol. Neurosci. 30, 137–159.
Tass, P.A., Qin, L., Hauptmann, C., Doveros, S., Bezard, E., Boraud, T., Meissner, W.G., 2012b. Coordinated reset neuromodulation has sustained effects in parkinsonian non-human primates. Ann. Neurol. 72, 816–820.
Vanneste, S., Plazier, M., Van der Loo, E., De Heyning, P., Congedo, M., De Ridder, D., 2010. The neural correlates of tinnitus-related distress. Neuroimage 52, 470–480.
Vanneste, S., Plazier, M., Ost, J., Van der Loo, E., De Heyning, P., De Ridder, D., 2011. Bilateral dorsolateral prefrontal cortex modulation for tinnitus by transcranial direct current stimulation: a preliminary clinical study. Exp. Brain Res. 202, 779–785.
Vanneste, S., Joos, K., De Ridder, D., 2012. Prefrontal cortex based sex differences in tinnitus perception: same tinnitus intensity, same tinnitus distress, different mood. PLoS One 7, e31182. http://dx.doi.org/10.1371/journal.pone.0031182.
Voisin, J., et al., 2006. Listening in silence activates auditory areas: a functional magnetic resonance imaging study. J. Neurosci. 26, 273–278.
Weisz, N., Moratti, S., Meinzer, M., Dohrmann, K., Elbert, T., 2005. Tinnitus perception and distress is related to abnormal spontaneous brain activity as measured by magnetoencephalography. PLoS Med. 2, e153. http://dx.doi.org/10.1371/journal.pmed.0020153.
Weisz, N., Hartmann, T., Dohrmann, K., Schlee, W., Norena, A., 2006. High-frequency tinnitus without hearing loss does not mean absence of deafferentation. Hear. Res. 222, 108–114.
Weisz, N., Dohrmann, K., Elbert, T., 2007a. The relevance of spontaneous activity for the coding of the tinnitus sensation. Prog. Brain Res. 166, 61–70.
Weisz, N., Muller, S., Schlee, W., Dohrmann, K., Hartmann, T., Elbert, T., 2007b. The neural code of auditory phantom perception. J. Neurosci. 27, 1479–1484.
Weisz, N., Hartmann, T., Mueller, N., Lorenz, I., Obleser, J., 2011. Alpha rhythms in audition: cognitive and clinical perspectives. Front. Psychol. 2. http://dx.doi.org/10.3389/fpsyg.2011.00073.
Yang, S., Weiner, B.D., Zhang, L.S., Cho, S.J., Bao, S., 2011. Homeostatic plasticity drives tinnitus perception in an animal model. Proc. Natl. Acad. Sci. U. S. A. 108, 14974–14979.
Yukie, N., 1995. Neural connections of auditory association cortex with the posterior cingulate cortex in the monkey. Neurosci. Res. 22, 179–187.
Yuste, R., Bonhoeffer, T., 2004. Genesis of dendritic spines: insights from ultrastructural and imaging studies. Nat. Rev. Neurosci. 5, 24–34.